Universidade Nova de Lisboa

Instituto de Higiene e Medicina Tropical

Detection and phylogenetic analysis of tick-borne viruses circulating in Portugal and Poland

Sara Margarida Martins Afonso

DISSERTAÇÃO PARA OBTENÇÃO DO GRAU DE MESTRE EM MICROBIOLOGIA MÉDICA

JULHO, 2023

Universidade Nova de Lisboa

Instituto de Higiene e Medicina Tropical

Detection and phylogenetic analysis of tick-borne viruses circulating in Portugal and Poland

Autor: Sara Margarida Martins Afonso

Orientador: Professor Doutor Ricardo Parreira

Coorientador: Doutora Sandra Antunes

Dissertação apresentada para cumprimento dos requisitos necessários à obtenção do grau de Mestre em Microbiologia Médica

2022/2023	Sara M. M. Afonso	Detection and phylogenetic analysis of tick-borne viruses circulating in Portugal and Poland

“I am going to write a little Book for Murray on orchids, and today I hate them worse than everything.”

— Charles Darwin, 1861, in a letter to his friend Charles Lyell

ACKNOWLEDGEMENTS

I would like to express my gratitude to everyone who supported me during this project, namely:

Prof. Dr. Ricardo Parreira, for your active supervision of my project, as well as your infinite patience and willingness to accommodate any last-minute changes of plans due to my status as a working student.

Dr. Sandra Antunes, for co-supervising my project, and always being available to help and discuss any issues.

Prof. Dr. João Piedade, for accepting me in this Masters programme and encouraging me throughout my journey.

Dr. Will Allen (Swansea University) for expressing interest in my work for Sensory Ecology, it was the first time I felt truly seen and appreciated for my efforts.

Dr. Penny Neyland, Dr. Laura Roberts, and Dr. Almudena Ortiz-Urquiza for being great role models and inspiring me to become a well-rounded woman in academia.

Dr. Fowler, Dr. Rory Wilson, Dr. Ed Pope, and Dr. Andrew King for being outstanding lecturers and story-tellers, as well as for the practical life/work advice to stay on top of the game.

Dr. Ashley Levine for teaching me everything about scientific writing and literature search, we often take these skills for granted but they are so important.

Elisa Granato for showing me that sense of humour has a place in academia.

D. Cila for taking me in the coffee shop and allowing me to finance my studies. To Jacira Fernandes, Renata Ayubi, and Liliana Lima, some of the most beautiful and hardworking women I have ever met, for the honest conversations in the coffee shop.

André Santos, Beatriz Lotra, Carolina Bernardino, and Sarah Gothe for the occasional get-togethers keeping us sane, and conversations about our future.

Connie Klaver for being a great housemate and not getting mad at me for neglecting the houseplants.

Dr. Renke Lühken for taking me in a PhD programme and giving me the time to settle in Germany while finishing my Master's thesis. To Felix, Leif, Magda, Pride, Tatiana, and Timmy, for being wonderful colleagues and guiding me through my first year working at the BNI.

My dearest friend Konstanza Woźniacka, a constant source of strength and inspiration, I would not be where I am right now if it was not for you.

My brother, my grandparents, and my wonderful mother, for their love and support.

RESUMO

As carraças são vetores de diversos agentes infecciosos, incluindo o notório vírus da encefalite transmitida por carraças (TBEV), o vírus Heartland (HRTV), membro da família *Phenuiviridae*, e os recentemente descobertos jingmenvírus, como o vírus Jingmen (JMTV) e o vírus Alongshan (ALSV). A vigilância epidemiológica molecular é crucial não só para compreender a diversidade dos vírus circulantes, mas também no que toca à prevenção e contenção de surtos. Uma vez que os estudos que caracterizam o viroma das carraças de Portugal são escassos, o objetivo deste projeto consiste em rastrear carraças colhidas em Portugal para a deteção de jingmenvírus e flebovírus, concluíndo com a análise filogenética das sequências resultantes. Um protocolo de RT-PCR dedicado e primers desenhados internamente foram utilizados nos ensaios para a detecção de jingmenvírus. Adicionalmente, extratos previamente disponibilizados de cDNA de carraças da Polónia foram rastreados para flebo- e jingmenvírus, assim como flavivírus. Os resultados mostraram que os flebovírus, particularmente os da linhagem AnLuc, circulam com uma prevalência elevada de 29% (10 *pools* positivos em 35) em carraças *Rhipicephalus bursa* das regiões de Lisboa e Alentejo de Portugal, de acordo com estudos anteriores realizados no Instituto de Higiene e Medicina Tropical (IHMT). O vírus Uukuniemi (UUKV) foi ainda detetado com uma prevalência surpreendentemente alta de 12% (quatro *pools* positivos em 34) em *Ixodes ricinus* da província de Warmińsko-Mazurskie na Polónia, o que sugere que o UUKV é altamente endémico nessa região. As sequências nucleotídicas partilham 98,7% de identidade com sequências de UUKV isoladas entre 1963 e 2004, o que demonstra que o UUKV tem um genoma de RNA particularmente estável. Não foram detetados jingmenvírus ou flavivírus nos espécimes de ambos os países, o que pode refletir a baixa diversidade espacial, temporal e taxonómica das amostras de carraças rastreadas, limitações inerentes à abordagem de amplificação com *primers* específicos ou, eventualmente, baixa prevalência ou, simplesmente, ausência destes grupos virais nas regiões investigadas.

Palavras-chave: vírus transmitidos por ixodídeos; *Flavivirus*; *Phlebovirus*; análise filogenética; rastreio epidemiológico

ABSTRACT

Ticks are vectors of many infectious agents, including the notorious tick-borne encephalitis flavivirus (TBEV), the *Phenuiviridae* member Heartland virus (HRTV), and novel flavi-like viruses of the Jingmen group, such as Jingmen tick virus (JMTV) and Alongshan virus (ALSV). Molecular epidemiology surveys are important not only to gain a good understanding of the diversity of circulating viruses, but also in outbreak prevention and preparedness. Since the virome of ticks from Portugal remains poorly understood, this study aimed to screen ticks collected in Portugal for flavi-like viruses and phleboviruses, the latter known to circulate in the country, and use phylogenetic tools to analyse the resulting sequences. A dedicated nested RT-PCR protocol and *in-house* designed primers were used in assays for the detection of Jingmen group viruses. In addition, available cDNA extracts of ticks from Poland were also surveyed for phlebo- and jingmenviruses, as well as flaviviruses. Results showed that phleboviruses, particularly those of the AnLuc lineage, circulate with a high prevalence of 29% (10 positives in 35 pools) in *Rhipicephalus bursa* questing ticks from the Lisboa and Alentejo regions of Portugal, in accordance with previous studies carried out at Instituto de Higiene e Medicina Tropical (IHMT). Additionally, the Uukuniemi virus (UUKV) was detected with a surprisingly high prevalence of 12% (four positives in 34 pools) in *Ixodes ricinus* from the Warmińsko-Mazurskie province in Poland, suggesting that UUKV is highly endemic to this area. Sequences shared 98.7% nucleotide identity with UUKV strains isolated between 1963 and 2004, which demonstrates that UUKV has a remarkably stable RNA genome. No jingmenviruses or flaviviruses were detected in the specimens from either country, which could reflect the low spatial, temporal, and taxonomic diversity of the tick samples surveyed, limitations inherent to the targeted approach or, eventually, low prevalence or, simply, absence of these viral groups in these regions.

Keywords: tick-borne viruses; *Flavivirus*; *Phlebovirus*; phylogenetic analysis; epidemiological survey

INDEX

LIST OF ABBREVIATIONS

ALKV	Alkhurma virus
ALSV	Alongshan virus
ASFV	African swine fever virus
BHAV	Bhanja virus
BLAST	Basic local alignment search tool
BLASTn	Nucleotide basic local alignment search tool
bp	Base pairs
°C	Degree Celsius
CCHFV	Crimean-Congo haemorrhagic fever virus
CDC	Centers for Disease Control and Prevention
cDNA	Complementary DNA
$CHCl_3$	Chloroform
DNA	Deoxyribonucleic acid
DNase	Deoxyribonuclease
dNTP	Deoxyribonucleotide triphosphate
DMEM	Dulbecco's modified Eagle's medium
ECDC	European Centre for Disease Prevention and Control
EDTA	Ethylenediaminetetraacetic acid
EVOA	Espaço de Visitação e Observação de Aves
FoFiSpp1F, RoRiSpp1R	Hybrid primers containing SPP1 sequence used to assemble positive control for the detection of Jingmenviruses
g	Gram (SI unit)
GCXV	Guaico Culex virus
GPS	Global positioning system
h	Hour
HIGV	Hunter Island group virus
H_2O	Water (chemical formula)
HRTV	Heartland virus
IHMT	Institute of Hygiene and Tropical Medicine
IPTG	Isopropyl-ß-D-thiogalactopyranoside
JMTV	Jingmen tick virus
K^+	Potassium ion
KAMV	Kabuto Mountain virus
KITV	Kindia tick virus
L	Litre (SI unit)
LB	Lysogeny broth medium
LIV	Louping-ill virus
LSV	Lone star virus
M	Molar concentration (mol/L = mol/dm^3)
MAFFT	Multiple alignment using fast Fourier transform
mg	Milligram
Mg^{2+}	Magnesium ion
MGTV	Mogiana tick virus
min	Minute
ML	Maximum likelihood
mL	Millilitre
mol	Mole (SI unit)
NA	Not applicable
NaOAc	Sodium acetate
NaOH	Sodium hydroxide
NCBI	National Center for Biotechnology Information
NGS	Next-generation sequencing
NJ	Neighbour Joining method

NS3, NS5	Non-structural proteins 3 and 5, respectively, of flaviviruses
NSDV	Nairobi sheep disease virus
NSP1, NSP2	Non-structural proteins 1 and 2, respectively, of JMTV
NTV	Newport tick virus
OHFV	Omsk haemorrhagic fever virus
ORF	Open reading frame
PCR	Polymerase chain reaction
p	"Pico-" prefix, i.e., 10^{-12}
pfu	Plaque forming units
pmol	Picomole
POWV	Powassan virus
ppL1, ppL2	Primer sets targeting portion of the *Phenuiviridae* L-segment
RNA	Ribonucleic acid
RNase	Ribonuclease
rpm	Revolutions per minute
RT-PCR	Reverse transcription polymerase chain reaction
s	Second (SI unit)
SDS	Sodium dodecyl sulfate
S1, S2, S3, S4	Segments 1, 2, 3, and 4, respectively, of the JMTV genome
SFSV	Sicilian virus
SFTSV	Severe fever with thrombocytopenia syndrome virus
SHIV	Shuangao insect virus
SOC	Super Optimal broth with Catabolite repression medium
SPP1	*Bacillus subtilis* bacteriophage SPP1
TAHV	Tahyna orthobunyavirus
TAKV	Takachi virus
TBD	Tick-borne disease
TBE	Tick-borne encephalitis
TBEV	Tick-borne encephalitis virus
TBPV	Tick-borne phlebovirus
TE	Tris-EDTA buffer
TEG	Triethylene glycol
T_m	Primer melting temperature
Tris-HCl	Tris (hydroxymethyl) aminomethane (THAM) hydrochloride
TOSV	Toscana virus
TOYOV	Toyo virus
TSS	Transformation and storage solution
UUKV	Uukuniemi virus
USA	United States of America
UTR	Untranslated region
V	Volt (SI unit)
WHAV	Wuhan aphid virus
WNV	West Nile virus
w/v	Weight per volume
X-gal	5-Bromo-4-chloro-1H-indol-3-yl β-D-galactopyranoside
YGTV	Yanggou tick virus
µ	"Micro-" prefix, i.e., 10^{-6}
µg	Microgram
µL	Microliter
1NS5F/1NS5Re, 2NS5F/2NS5Re	Primer sets targeting the NS5 gene of *Flavivirus* (first and second round primers, respectively)

INTRODUCTION

1. Tick diversity and relevance of tick-borne diseases (TBDs)

As obligate haematophagous ectoparasites, ticks are vectors of a diverse range of infectious agents that play an important role as the underlying cause of disease in humans and domestic animals, with extensive impact on public health and economy (Kazimírová et al., 2017). Ticks are well-known for their promiscuous feeding behaviour which, combined with changes in global socio-economic and climatic conditions, as well as a lack of efficient control measures, are factors that contribute to their expanding geographical range. As a result, ticks are effective vehicles for the spread of various pathogens, including bacteria, nematodes, protozoa, and viruses, across all continents except for Antarctica (Brackney & Armstrong, 2016; Brites-Neto et al., 2015; Kazimírová et al., 2017).

All ticks share common ancestry and, therefore, form a monophyletic cluster in phylogenetic trees. Altogether, they comprise three families, Ixodidae, Argasidae, and Nuttalliellidae, belonging to the order Ixodida. Members of the Ixodidae family, commonly known as hard ticks, include 702 species characterised by terminal mouthparts and a chitin scutum totally or partially covering their dorsum (Brites-Neto et al., 2015). Although most zoonotic tick-borne diseases (TBDs) are transmitted by hard ticks, soft ticks of the Argasidae family may also act as TBD vectors (Dantas-Torres et al., 2012). With 193 described species, the Argasidae family is easily identified through its ventrally-positioned mouthparts and absent scutum, with important members including the genus *Ornithodoros* spp., implicated in the transmission of relapsing fever borreliae (Talagrand-Reboul et al., 2018), *Coxiella burnetti*, the causative agent of Q fever (Duron et al., 2015), and the haemorrhagic fever agent Alkhurma virus (ALKV) (Charrel et al., 2007). Finally, the Nuttalliellidae family is comprised by a single species, *Nuttalliella namaqua*, restricted to southern Africa and with no known association to disease (Keirans et al., 1976). Due to its morphology and basal phylogenetic position in relation to Argasidae and Ixodidae, *Nu. namaqua* was believed to be the closest relative to tick ancestors and the evolutionary "missing link" between other extant tick families (Mans et al., 2011), although this was later questioned by studies carried out with different molecular markers (Mans et al., 2012; Burger et al., 2014). Interestingly, two extinct tick families, Deinocrotonidae and Khimairidae, were recently described from a collection of specimens preserved in 100-million-year-old amber from Myanmar (Southeast Asia), suggesting that tick biodiversity and distribution in Gondwana was greater than estimated to date and re-igniting the debate regarding the exact spatio-temporal origin of ticks (Chitimia-Dobler et al., 2022; Dantas-Torres, 2018; Peñalver et al., 2017).

Notwithstanding the uncertainty regarding their origin and patterns of dispersal, ticks are currently widespread around the world and carry a myriad of pathogens associated with diseases of high medical and veterinary importance, including tick-borne encephalitis, Crimean-Congo haemorrhagic fever, and Lyme disease (**TABLE 1**). Lyme disease is by far the most prevalent tick-borne disease in the northern hemisphere, with 476,000 new cases per year in the US alone (Global Lyme Alliance, 2023). A conservative estimation based on 42,743 cases reported in 2017 to the Centers for Disease Control and Prevention (CDC) resulted in USD $500 million spent annually in patient diagnose and treatment for Lyme disease, posing a significant burden on the country's economy (Adrion et al., 2015; Rochlin & Toledo, 2020). As for their veterinary impact, tick-borne diseases can affect up to 80% of cattle worldwide, with economic losses of USD $364 million and a mortality of 1.3 million cattle estimated for countries such as Tanzania, for instance, mostly due to theileriosis, anaplasmosis and babesiosis (Kivaria, 2006; Rochlin & Toledo, 2020). Tick-borne flaviviruses, notable for causing encephalitis and haemorrhagic symptoms, are yet another source of concern for public health and economy, leading to 100,000 hospitalisations in Europe, Russia, China and Japan (Heinz & Holzmann, 2001). Most importantly, recent trends show an increase in the geographical range and number of human cases caused by tick-borne viral diseases, as demonstrated by the expansion of tick-borne encephalitis virus (TBEV) across Europe and the rise of Powassan virus (POWV), once an obscure pathogen in northeastern North America, across North America and Eurasia (Hermance & Thangamani, 2017; Mansfield et al., 2017).

TABLE 1. Medically relevant examples of tick-borne diseases (TBDs) across the globe. Number of human cases reported per year according to most recent data from ECDC or CDC annual reports (country-specific data presented where global statistics are unavailable). References: Brites-Neto et al., 2015; CDC, 2021; CDC, 2022b; Colwell et al., 2011; Domínguez et al., 2020; ECDC, 2022a; Gern et al., 1998; NYC Government, 2023; Santos, 2014; Sood et al., 2011; Spernovasilis et al., 2021; Tsergouli et al., 2020; WHO, 2023.

Disease	Pathogen	Affected regions	Main tick vectors	Vertebrate reservoirs	Number of human cases reported annually
Babesiosis	*Babesia* spp. (protozoan)	North America and Europe	*Ixodes ricinus, Ixodes scapularis, Rhipicephalus (Boophilus) microplus*	Cattle, roe deer, rodents	2,418 cases in North America
Crimean-Congo haemorrhagic fever	Crimean-Congo haemorrhagic fever virus (CCHFV; *Orthonairovirus*)	Southern Asia, Northern Africa, Southern Europe	*Hyalomma marginatum* (other *Hyalomma* species also competent), *Rhipicephalus bursa*	Small mammals are amplifying hosts. Infection of humans usually through contact with livestock (ruminants, ostriches)	10,000-15,000 cases worldwide (500 fatal)
Lyme disease	*Borrelia burgdorferi* complex (bacteria)	America, Eurasia	*Ixodes* spp. (especially *I. ricinus* in Europe and I. *scapularis* in North America)	Small mammals (rodents), birds	476,000 cases in US
Mediterranean spotted fever	*Rickettsia conorii conorii* (bacteria)	Mediterranean basin	*Rhipicephalus sanguineus*	Canines, rabbits	140 cases in Portugal
Powassan virus disease	Powassan virus (POWV; *Flavivirus*)	North America, eastern Russia	*Dermacentor andersoni*, *D. variabilis*, *Ixodes cookie*, *I. scapularis*	Small mammals (rodents), medium sized mammals (skunks, raccoons)	20 cases in North America
Rocky Mountain spotted fever	*Rickettsia rickettsii* (bacteria)	America	*Dermacentor variabilis* and *D. andersoni* in North America, *Amblyomma cajannense* in Central and South America	Rodents, rabbits, and dogs	250-1,200 cases in the US
Tick-borne encephalitis	Tick borne encephalitis virus (TBEV; *Flavivirus*)	Europe, northern Asia (Russia, Siberia, China, Japan)	*I. ricinus* in Europe and *I. persulcatus* in northern Asia	Rodents, ruminants, dogs	10,000-12,000 cases worldwide
Tick-borne relapsing fever	*Borrelia spp.* (bacteria)	Africa, Iberian Peninsula, Saudi Arabia, Asia, North America	*Ornithodoros* spp.	Rodents	6 cases in Spain

Tick-borne viruses (TBVs) are genetically heterogeneous and became a subject of research interest when some members were associated with severe disease and high mortality rates in humans. All TBVs pathogenic to humans are zoonotic, that is, the virus is maintained in a sylvatic cycle between wild animals (vertebrates) and vectors (invertebrates), wherein humans rarely contribute to circulation but may be infected as dead-end hosts (Jahfari & Sprong, 2016; Kazimírová et al., 2017). Apart from African swine fever virus (ASFV), the sole member of family *Asfarviridae* and the only known DNA

arbovirus, TBVs are generally categorised into eight RNA viral families (**FIGURE 1**) (Gaudreault et al., 2020; Shi et al., 2018). Almost 25% of TBVs have been linked to illness, with members of high medical and/or veterinary importance ranging from flaviviruses (genus *Flavivirus*, family *Flaviviridae*) such as tick-borne encephalitis virus (TBEV) and Powassan virus (POWV), to orthonairoviruses (genus *Orthonairovirus*, family *Nairoviridae*) like the Crimean-Congo haemorrhagic fever virus (CCHFV) and Nairobi sheep disease virus (NSDV), as well as bandaviruses (genus *Bandavirus*, family *Phenuiviridae*), particularly severe fever with thrombocytopenia syndrome virus (SFTSV) and Heartland virus (HRTV) (Mansfield et al., 2017; Dinçer et al., 2022).

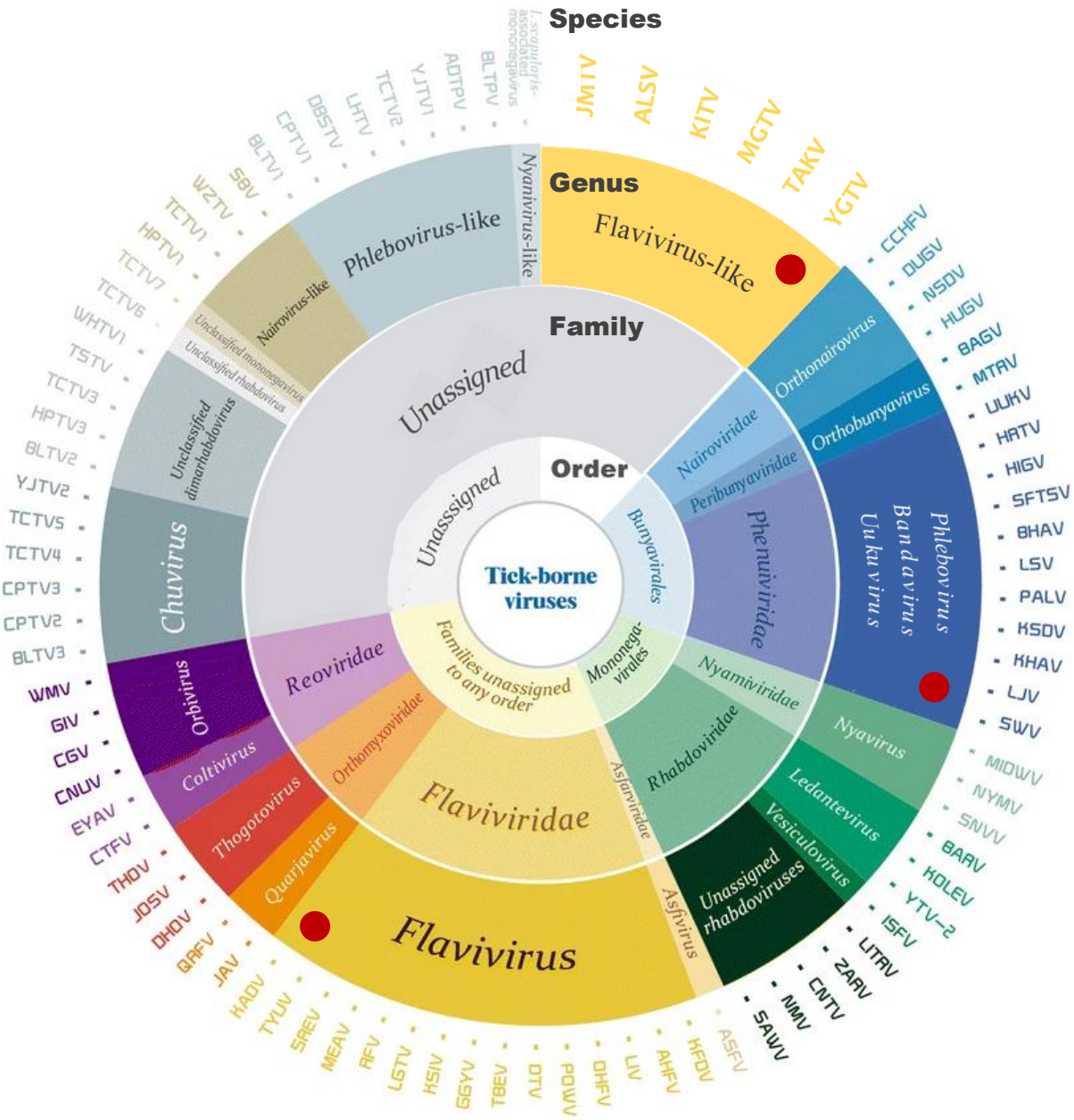

FIGURE 1. Taxonomy of tick-borne viruses. Adapted from Shi et al. (2018) and updated according to current ICTV taxonomy release (ICTV, 2022). Groups expanded upon in this study highlighted with a red circle.

2. Tick-borne viruses of the *Phenuiviridae* family

Until recently, TBVs of the *Phenuiviridae* family were encompassed within a single genus, *Phlebovirus*. Since 2018, they have mostly been shifted into two new genera, *Bandavirus* and *Uukuvirus*, with all three genera making up a total of 91 viral species (**FIGURE 1**) (ICTV, 2022). Unlike other negative-sense members of the order *Bunyavirales*, viruses of these genera follow an ambisense strategy in one of their three segments, the S segment encoding for the N (nucleoprotein) and NSs (non-structural) proteins (Walter & Barr, 2011). Most phleboviruses are transmitted by sandflies (e.g., Toscana and Naples viruses) and mosquitoes (e.g., Rift Valley fever and Gouleako viruses), whereas bandaviruses and uukuviruses are mainly tick-borne (Calisher & Calzolari, 2021).

The isolation of the Bhanja virus in 1954 from *Haemaphysalis intermedia* ticks in India marks the first instance of detection of a tick-borne phlebovirus (TBPV; here the acronym is used in a broad sense to denote all tick-borne viruses of the *Phenuiviridae* family, not only those of the *Phlebovirus* genus) (Shah & Work, 1969). Despite decades of neglect, TBPVs have garnered more attention in recent years with the discovery of SFTSV and HRTV in patients from China and the United States, respectively, exhibiting severe fever, thrombocytopenia, and leukocytopenia accompanied with gastrointestinal symptoms, chills, joint pain, and myalgia (Fang et al. 2015; Yu et al. 2011). Although mortality rates reach 15-50% for SFTSV disease and 10% for HRTV disease, there are currently no specific therapeutic agents available or licensed vaccines, but candidates for the latter have been proposed (Fujii et al., 2022; Kwak et al, 2019; Li et al., 2022; Sun et al., 2021). SFTSV and HRTV belong to the same phylogenetic group, the SFTS/Heartland group (**FIGURE 2**) (Matsuno et al., 2015). SFTSV was first detected in 2009 in an outbreak that affected 171 patients from six provinces of China (Xu et al., 2011). Towards the end of 2012, SFTSV infection had spread into another 11 Chinese provinces, standing at around 2,047 reported cases between 2011 and 2012 (Li et al., 2015b). The virus has since been reported in Japan, North and South Korea, USA, Taiwan, and many other countries (Sharma & Kamthania, 2021). Migration from different locations may have led to recombination and reassortment among SFTSV strains, explaining the observed association between SFTVS genotypes and their geographic distributions (Liu et al., 2014; Shi et al., 2017). HRTV shares 60-70% genetic similarity with SFTSV and was first isolated in the USA, in patients exhibiting the same symptoms as those induced by SFTSV (McMullan et al., 2012). To date, over 50 cases of human HRTV infection have been reported, all in the USA, where *Amblyomma americanum* ticks play a role as primary vectors (CDC, 2022a). Other viruses in the same phylogenetic group, such as the Hunter Island group virus (HIGV), have not been associated with disease.

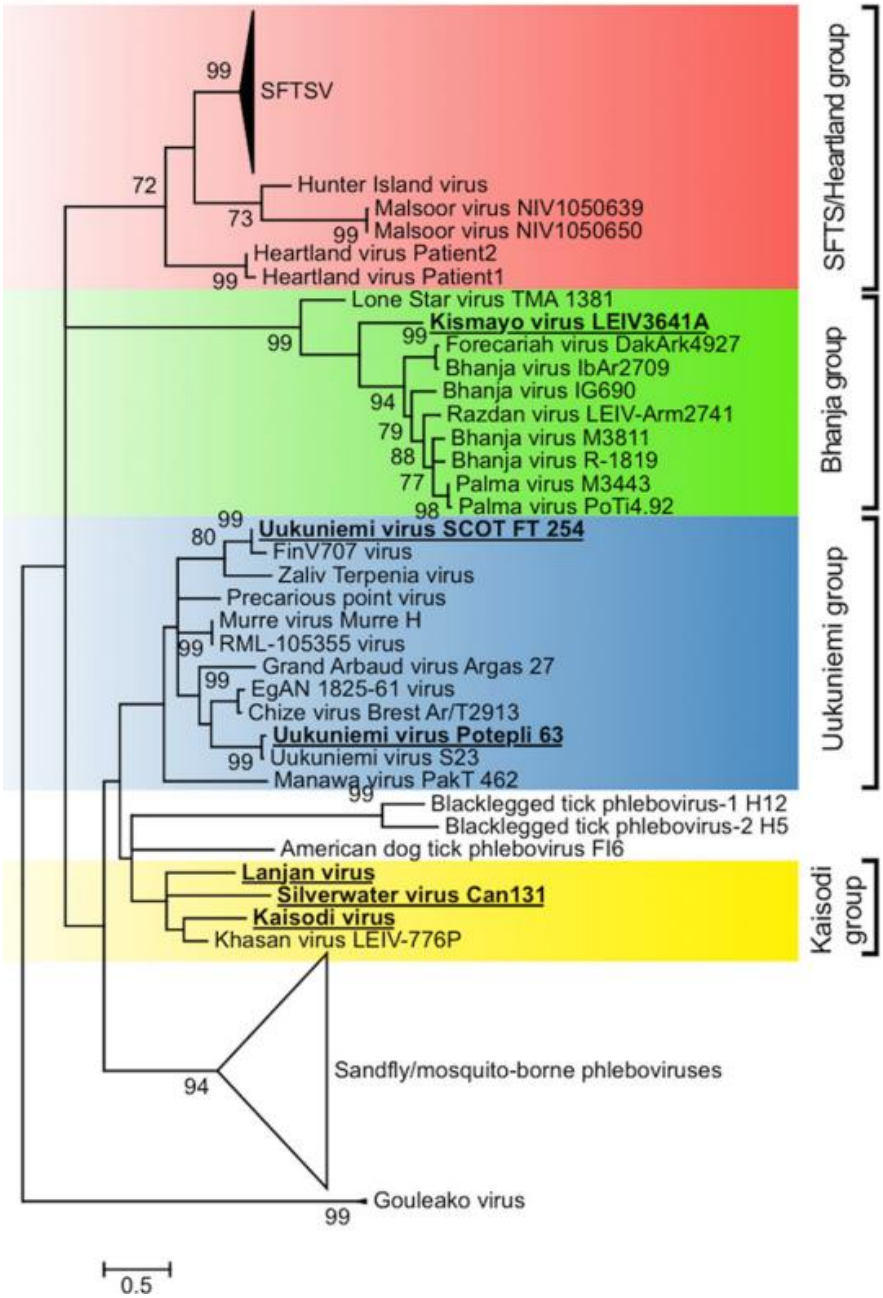

FIGURE 2. Phylogenetic tree based on a common 500-bp sequence (within the L segment) shared by phleboviruses, bandaviruses and uukuviruses, constructed using the maximum likelihood (ML) method with 1,000 bootstrap replicates. Bootstraps above 70% shown near the branches indicate strong topological support. Major phylogenetic groups formed by tick-borne sequences highlighted in red (SFTS/Heartland group), green (Bhanja group), blue (Uukuniemi group), and yellow (Kaisodi group). **Reference**: Matsuno et al., 2015.

In addition to the SFTS/Heartland group, Matsuno et al. (2015) assigned other known TBPVs into three other phylogenetic groups, the Uukuniemi, Bhanja, and Kaisodi groups, named after their type species (**FIGURE 2**). Besides Uukuniemi virus (UUKV), the Uukuniemi group includes at least 16 other species, such as Murre, Grand Arbaud and Zaliv Terpenia, identified across Europe, Africa, Middle Asia, Australia, and America (ICTV, 2022; Palacios et al., 2013). Three years after its first isolation

from *Ixodes ricinus* ticks collected in southern Finland (Saikku & Brummer-Korvenkontio, 1973), multiple strains of UUKV were identified in the Czech Republic (Kolman et al., 1966). A later study demonstrated that the minimum infection rate of *I. ricinus* with UUKV was double than that with TBEV, implying that UUKV was widespread in the Czech Republic (Kolman & Husova, 1971). Subsequently, UUKV was isolated from ticks in Scandinavia, Central and Eastern Europe, and Azerbaijan (CDC, 2023). Although antibodies to some Uukuniemi group members were detected in humans, up to the present day there has been no association with disease and, therefore, the group was not deemed as a threat to public health (Palacios et al. 2013). In contrast, the Bhanja group includes the neurotropic Bhanja virus (BHAV), first isolated in India and then in Africa and Europe (Hubalek 1987a), known to be pathogenic to ruminants and humans (Balducci et al. 1970; Hubalek 1987b). Also a member of this phylogenetic group, the lone star virus (LSV) can infect human and monkey cells but no evidence for human infection has been reported (Labuda & Nuttall, 2004). Similarly, no infectious cases have been associated with members of the Kaisodi group (Shi et al., 2018).

3. Tick-borne viruses of the *Flaviviridae* family

Flaviviridae viruses have single-stranded positive RNA genomes encoding a polyprotein that is cleaved into 2-4 structural proteins and 7-9 non-structural proteins (Chambers et al., 1990) using a combination of virus as well as cellular-encoded proteases. *Flavivirus*, one of the four genera belonging to this family, comprehends a large group of arboviruses transmitted by mosquitoes, ticks, or specific arthropod vectors, capable of infecting a wide range of vertebrates, including humans (Simmonds et al., 2017). The most notorious tick-borne virus of this genus is the tick-borne encephalitis virus (TBEV), the etiological agent of a severe infectious disease that often manifests as meningitis, encephalitis, or meningoencephalitis. Other symptoms include muscle paralysis, difficulties in swallowing, and long-term sequelae associated with cognitive disfunction (e.g., memory impairment, difficulty in concentrating) (Marjelund et al. 2004; Solomon et al., 2007). TBE is endemic in several central, northern, and eastern European countries (**FIGURE 3**) (Beauté et al., 2018). The latest available Annual Epidemiological Report by the ECDC accounted for 3,734 confirmed cases of TBE in Europe in 2020, with the highest notification rates reported in Lithuania, Slovenia, and Czechia (24.3, 8.9 and 7.9 cases per 100,000 population, respectively) (ECDC, 2022b). As a non-endemic region where no cases have been reported, TBE surveillance in Portugal is not practiced in an annual basis by the ECDC, with no data available in the last annual epidemiological report for 2020 (Beauté et al., 2018; ECDC, 2022b). Although multiple highly effective vaccines are available in Europe, there are currently no specific antivirals approved for the treatment of TBE, and patient care is symptomatic and supportive (Poulos et al., 2022).

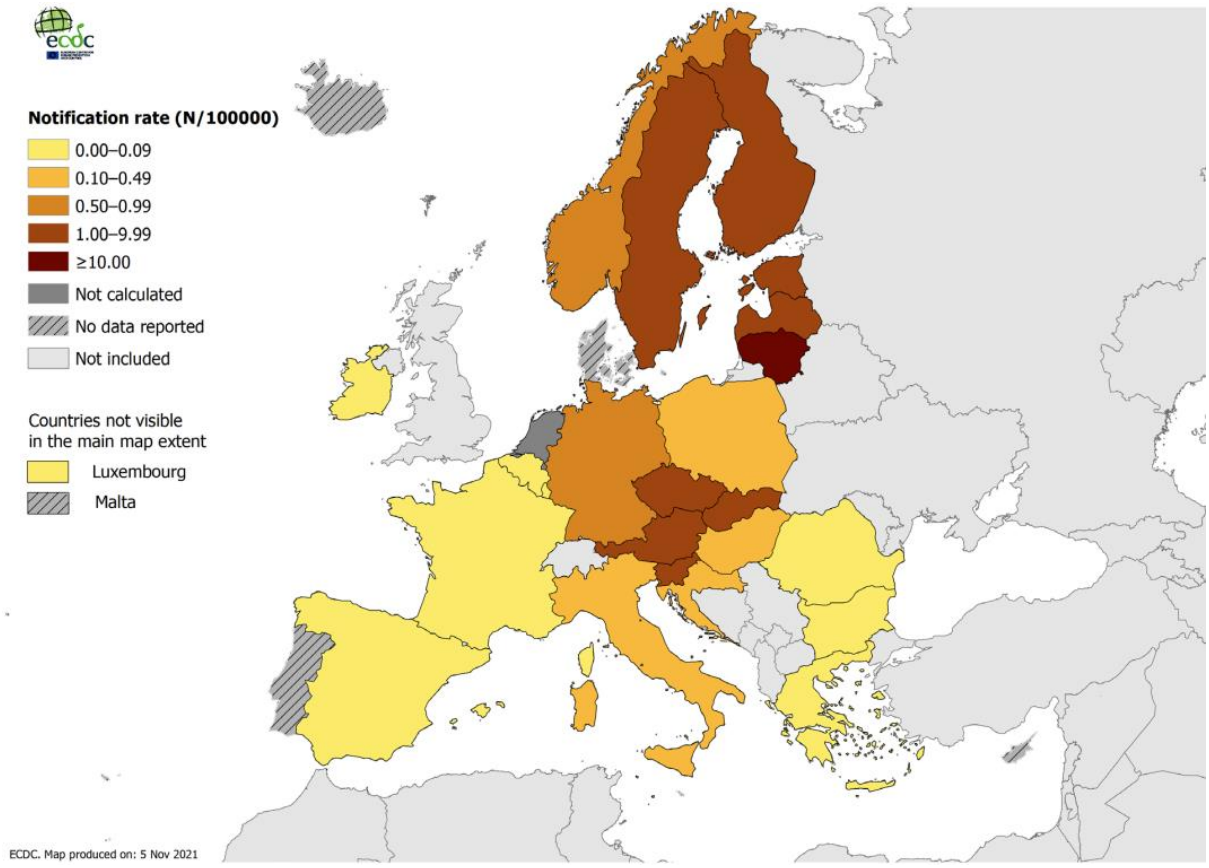

FIGURE 3. Distribution of confirmed tick-borne encephalitis cases per 100,000 population by country in EU/EAA, 2020. **Reference**: ECDC, 2022b

TBEV is classified into three subtypes associated with its geographic distribution in Europe and Russia (TBEV-Eu subtype), Siberia (TBEV-Sib subtype), or Far-Eastern Russia, China and Japan (TBEV-FE subtype) (Ecker et al., 1999). The main vector of TBEV-Eu is *I. ricinus*, while TBEV-Sib and TBEV-FE are transmitted by *I. persulcatus* (Süss, 2003), although at least eight tick species from three genera (*Ixodes*, *Dermacentor*, and *Haemaphysalis*) are known to be competent vectors for TBEV (Chitimia-Dobler et al., 2018; Ličková et al., 2020). TBEV is generally transmitted to ticks by co-feeding on infected rodents, which act as viral reservoirs (Randolph, 2011). Besides TBEV, other medically relevant tick-borne flaviviruses circulating in Europe include the louping-ill virus (LIV), mainly found in the British Islands (but also in Norway, Spain, Ireland, Turkey, and Bulgaria), the Powassan encephalitis virus (POWV), detected in North America and the Russian Far East, and Omsk haemorrhagic fever virus (OHFV), which occurs in parts of Russia (Beck et al., 2013). Despite their relevance as emerging pathogens, they are outside of the scope of this project and will not be expanded upon in this introduction.

4. Tick-borne viruses of the novel flavivirus-like Jingmen virus group

The accidental discovery of Jingmen tick virus (JMTV) in 2010 from a pan-phlebovirus RT-PCR of a pool of ticks collected in the Jingmen region of Hubei (China) changed our understanding of the genome structure and organisation of flaviviruses (Qin et al., 2014). The genome of JMTV is comprised of four segments, with segments S1 and S3 encoding two non-structural proteins (NSP1 and NSP2) that are genetically and functionally related to the flavivirus NS5 and NS3 sequences, respectively, whereas segments S2 and S4 encode three structural proteins (VP1, C and VP3) that share no known homology (**FIGURE 4**) (Vandegrift & Kapoor, 2019). Based on phylogenetic analyses, it is evident that the JMTV genome partly originated from an ancestral of the genus *Flavivirus* that "fragmented" to produce the individual NS3- and NS5-like segments (Qin et al., 2014). The other two segments were acquired independently from as-yet-unidentified parental ancestors (Vandegrift & Kapoor, 2019). JMTV was then the first known segmented RNA virus to have originated from an un-segmented virus.

In addition to representing a novelty from the genetic standpoint, another peculiar attribute that prompted JMTV to become a hot point in recent research was its ability to infect a broad range of ticks (**TABLE 2**) and insects, as well as mammals, including cattle, rodents, bats, and humans (Guo et al., 2020; Jia et al., 2019). Moreover, recent studies have detected JMTV in scorpions and even tortoises (Ogola et al., 2022; Paraskevopoulou et al., 2021), expanding our knowledge on JMTV host range. Most importantly, JMTV and the closely related Alongshan virus (ALSV) have been linked to cases of human febrile diseases in China and Kosovo (Li et al., 2015a; Zhang et al., 2020), and therefore are increasingly considered as a potential emerging threat to public health.

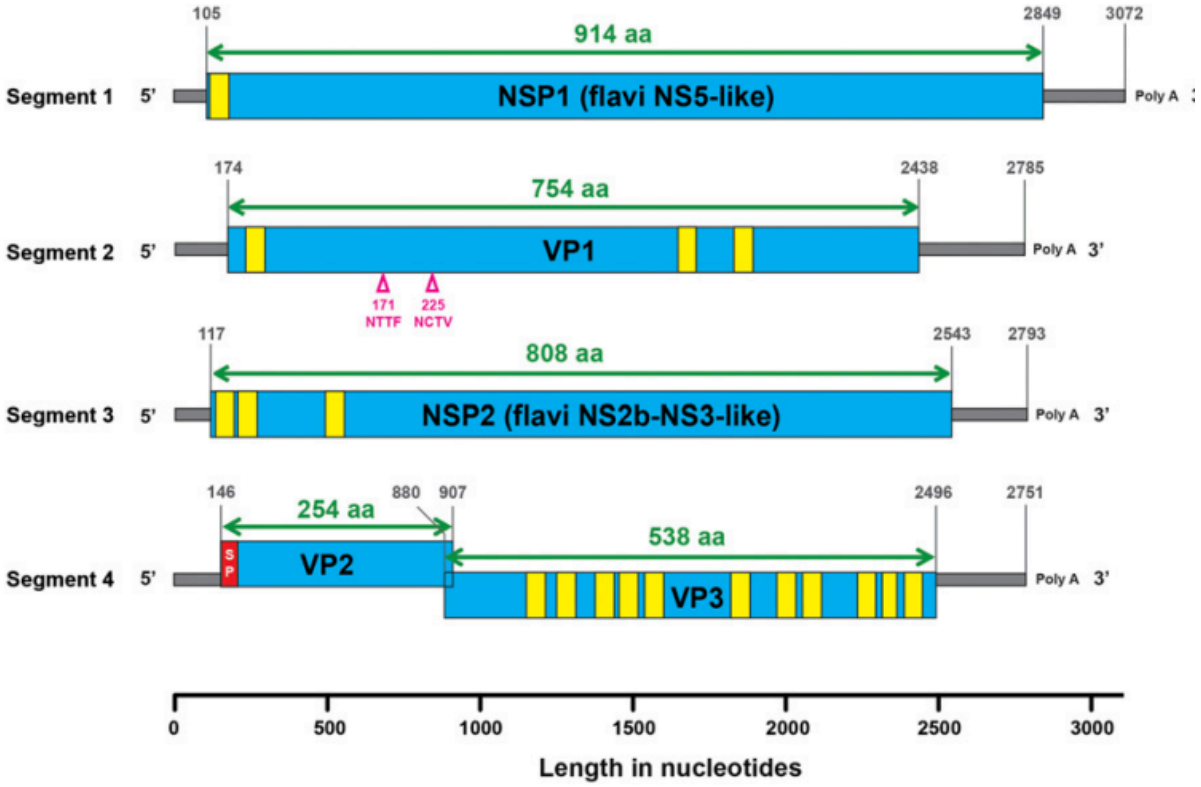

FIGURE 4. Genome organisation of and putative proteomic maps of JMTV, showing predicted ORFs (blue), transmembrane regions (yellow), signal peptides (red), and N-linked glycosylation sites (upward-pointing pink triangles). **Reference**: Qin et al., 2014.

TABLE 2. Tick species in which tick-associated Jingmen virus group species have been detected. **References**: Gondard et al., 2020; Kholodilov et al., 2021; Dinçer et al., 2019; Dinçer et al., 2022; Ogola et al., 2022; Zhang et al., 2020.

Tick genus	Tick species	Viruses detected			
		Jingmen tick virus (JMTV)	Alongshan virus (ALSV)	Mogiana tick virus (MGTV)	Yanggou tick virus (YTV)
Amblyomma	*javanense*	●			
	nuttalli	●			
	sparsum	●			
	testudinarium	●			
	variegatum	●			
Dermacentor	*marginatus*				●
	nuttalli		●		●
	reticulatus		●		
Haemaphysalis	*campanulata*	●			
	concinna		●		
	flava	●			
	hystricis	●			
	inermis	●			
	longicornis	●			
	parva	●			
Hyalomma	*marginatum*	●			
	truncatum	●			
Ixodes	*granulatus*	●			
	persulcatus		●		
	ricinus	●	●		
	sinensis	●			
Rhipicephalus	*appendiculatus*	●			
	bursa	●			
	evertsi evertsi	●			
	geigyi	●			
	microplus	●		●	
	sanguineus	●			
	turanicus	●			

JMTV and viruses with a similar genomic structure, collectively referred to as JMTV-like viruses or Jingmen virus group, have been identified in all continents except Antarctica (**FIGURE 5**) (Paraskevopoulou et al., 2021). In China, where it was first detected and described, JMTV has been found in at least 10 provinces, ranging from Xinjiang, to Heilongjiang, Zhejiang, and Yunan (Guo et al., 2020; Jia et al., 2019; Meng et al., 2019; Shi et al., 2021; Xu et al., 2020; Yu et al., 2020). In Europe, JMTV was detected in tick pools from France, Russia, and Serbia (Kholodilov et al., 2021; Stanojević

et al., 2020; Temmam et al., 2019). Notably, ALSV was identified in Finland from *I. ricinus* ticks, a common species across the entire extent of the European continent, highlighting the importance of molecular epidemiology surveys for TBV surveillance in Europe (Kuivanen et al., 2019).

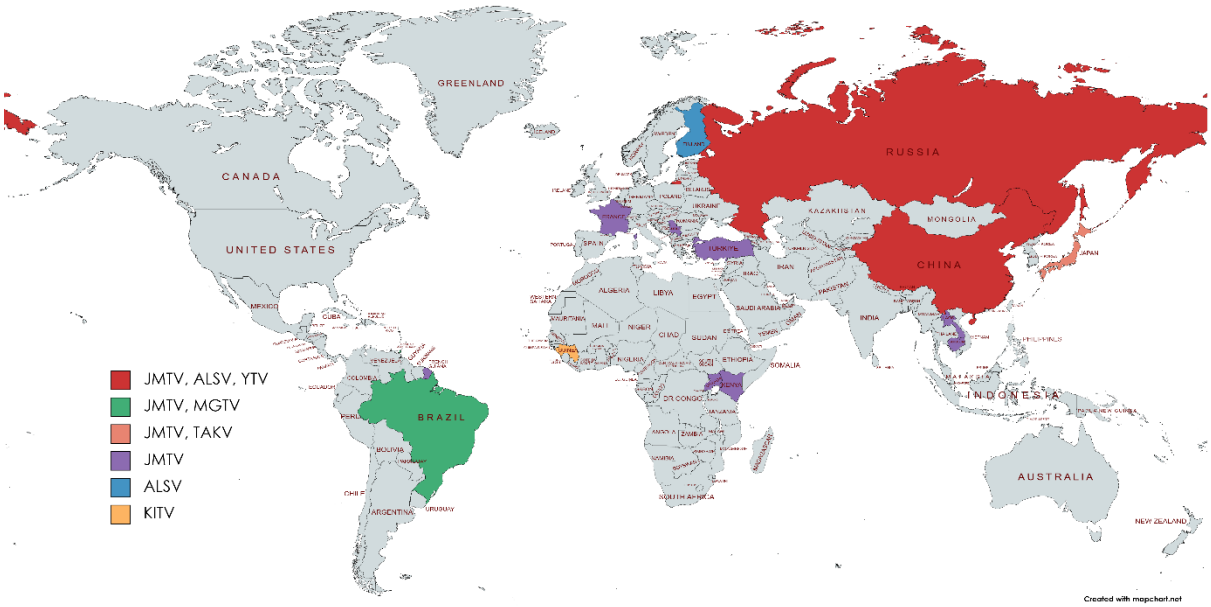

FIGURE 5. Countries in which Jingmen group viruses have been detected in ticks and/or mammals. Actual distribution within each country is not represented in this figure. **References**: Dinçer et al., 2019; Emmerich et al., 2018; Gondard et al., 2020; Guo et al., 2020; Kholodilov et al., 2021; Kobayashi et al., 2021a; Kuivanen et al., 2019; Ladner et al., 2016; Maruyama et al., 2014; Ogola et al., 2022; Pang et al., 2022; Sameroff et al., 2019; Stanojević et al., 2020; Temmam et al., 2019; Ternovoi et al., 2020; Wang et al., 2019.

Jingmen viruses cluster into two major phylogenetic groups, insect- and tick-associated Jingmen viruses (**FIGURE 6**). Insect-associated Jingmen viruses only infect arthropods, with examples including the Guaico Culex virus (GCXV), Wuhan aphid virus (WHAV), and Shuangao insect virus (SHIV) (Temmam et al., 2019). Tick-associated Jingmen viruses (otherwise known as arbo-Jingmenviruses) are transmitted by blood-feeding arthropods and encompass the vertebrate-pathogenic JMTV and ALSV, as well as other lesser-known members that have not been associated with pathogenic infection, such as Kindia tick virus (KITV), Mogiana tick virus (MGTV), Takachi virus (TAKV), and Yanggou tick virus (YGTV) (Ogola et al., 2022; Zhang et al., 2020). The insect- and tick-associated Jingmen viruses differ in a number of genetic features. For instance, conserved nucleotide stretches in the 5' and 3' untranslated regions (UTRs), as well as a 3'-end poly-A tail, are present in all four segments in tick-associated Jingmen viruses, but this is not the case for the insect-associated Jingmen viruses (Paraskevopoulou et al., 2020).

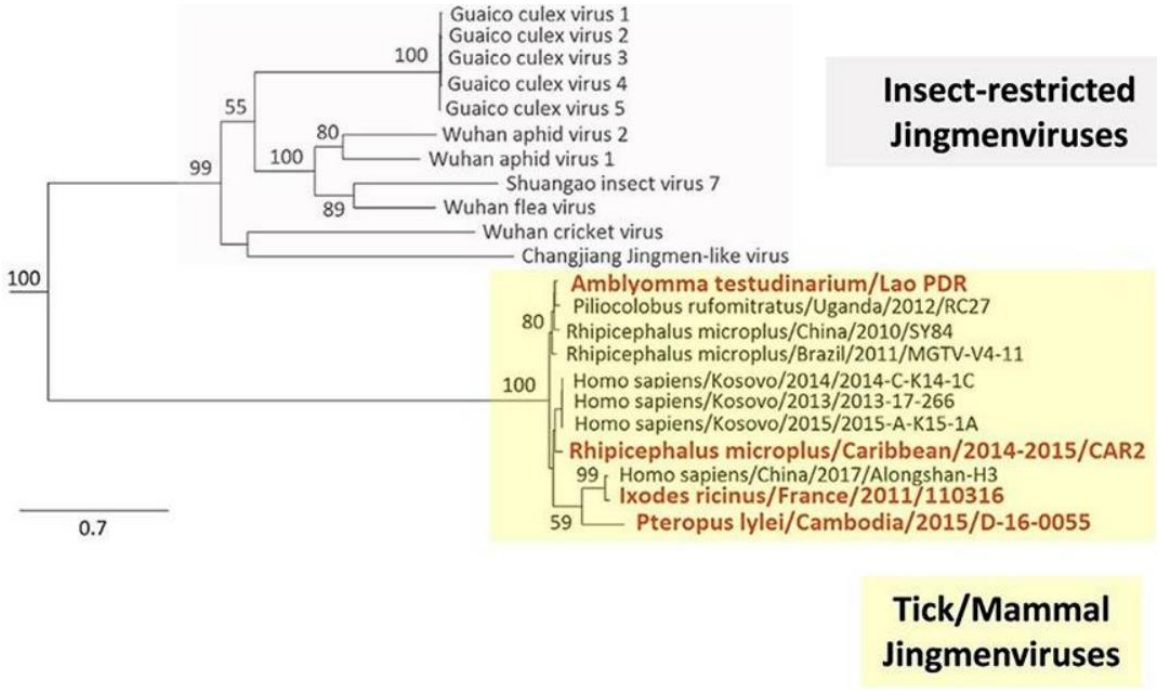

FIGURE 6. Maximum likelihood (ML) construction based on the complete RdRp amino acid sequence of Jingmen viruses. Major phylogenetic groups highlighted in grey (insect-associated Jingmen viruses) and yellow (tick-associated Jingmen viruses). **Reference**: Temmam et al., 2019.

Arbo-Jingmenviruses are split into at least three clades, A, B, and C, each clade containing tick-borne and mammal-borne viruses (**FIGURE 7**) (Temmam et al., 2019). Clade A is formed by tick-borne JMTV strains from China and Brazil, as well as JMTV strains isolated from bats and rodents from China, and a primate from Uganda. Tick-borne strains of KITV and MGTV detected in Guinea and Brazil, respectively, are also placed within clade A. Three sequences of Chinese tick-borne JMTV are embedded in the sub-clade of rodent-borne JMTV, suggesting frequent events of transmission between ticks and rodents, and thus a possible role for rodents as reservoirs (Temmam et al., 2019). Clade B is comprised of tick-borne JMTV from the French Antilles, Romania, Trinidad and Tobago, and Turkey, and human JMTV strains from human blood with origin in Kosovo. Lastly, clade C includes JMTV strains from *Ixodes* ticks in France, Finland and Russia, and a strain of human ALSV from China. In clade A, a lack of clustering according to tick species may be explained by frequent transmission of JMTV among tick species, facilitated by co-feeding on a same mammalian host (Shi et al., 2016b). Similarly, there appears to be no obvious segregation of JMTV strains according to geographical origin, indicating that dispersal over long distances has been a common occurrence throughout the evolution of this virus (Shi et al., 2016b). As hosts of several JMTV strains, bats may likewise have contributed to the widespread transmission of this virus, owing to their global distribution and abundance, large population densities, and ability to fly long distances (Guo et al., 2020).

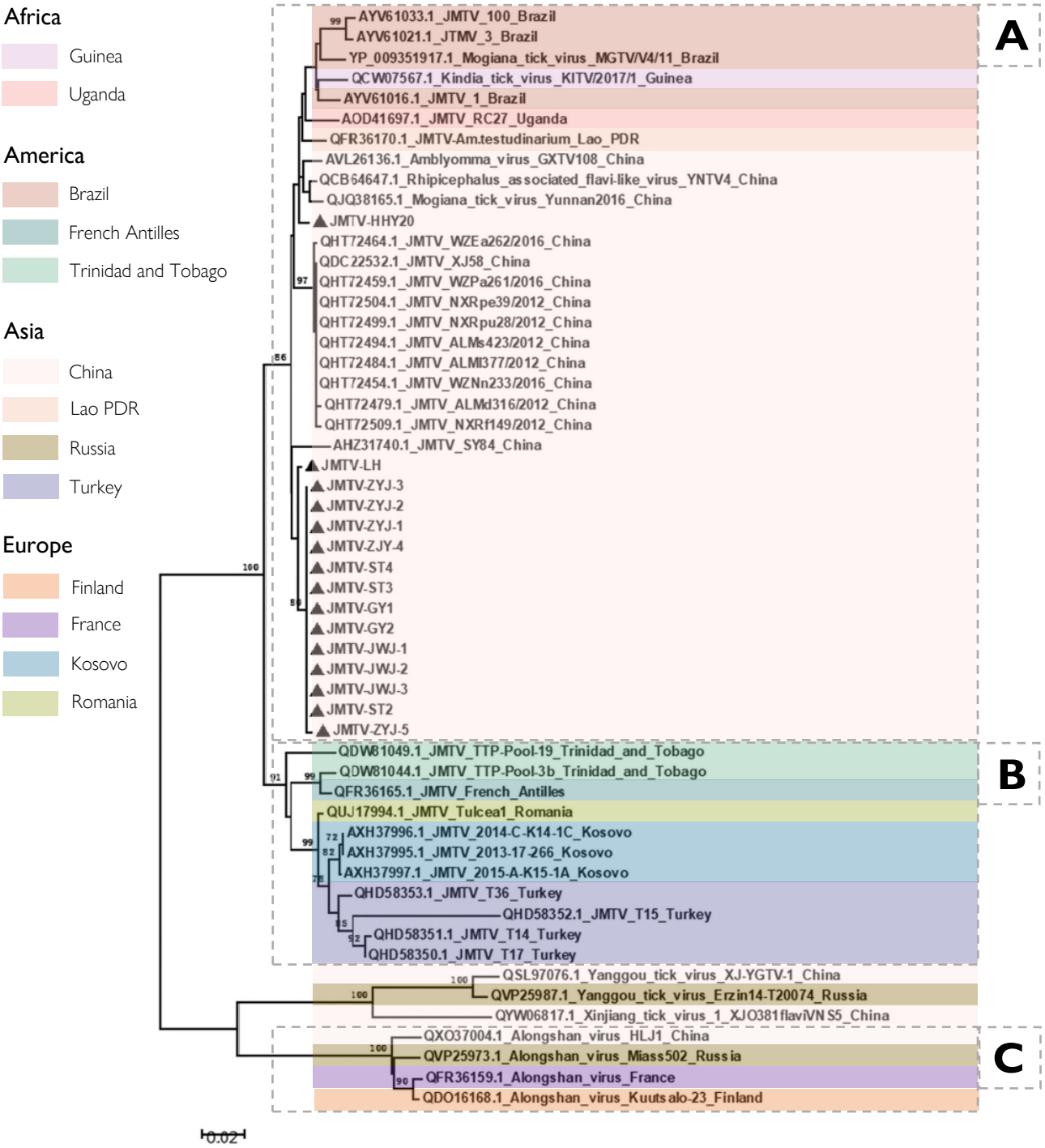

FIGURE 7. Phylogenetic analysis based on a 415-amino-acid fragment of NSP1 of Jingmen viruses using a Neighbour Joining (NJ) method, with 1,000 replicates and bootstrap values over 70% considered significant. Major phylogenetic groups (A, B, and C) represented in grey boxes. Sequence geographical origin highlighted according to colour-code in the figure. **References**: Guo et al., 2020; Pang et al., 2022.

5. Metagenomics as a window into the tick virome

Recent advances in high-throughput sequencing technology have boosted the discovery of novel phlebo-, rhabdo-, chu- and flavi-like viruses, although the degree of health risk they pose is still unclear (Brinkmann et al. 2018; Dinçer et al. 2019). For instance, a survey of tick-borne viruses in Hyogo, Japan, resulted in the identification of a novel member of the genus *Phlebovirus* designated as Kabuto Mountain virus (KAMV) (Ejiri et al., 2017). Phylogenetic analysis revealed that KAMV branches between the Uukuniemi and Kaisodi groups, thereby suggesting that KAMV is closely related to these two TBPV groups. Another newly discovered TBPV, Toyo virus (TOYOV), also originating from a tick pool collected in Japan during a surveillance assay, was found to belong to the Kaisodi group (46-70% sequence identity) (Kobayashi et al., 2021b). Even more recently, Newport tick virus (NTV) was one of 10 novel putative viral species identified in a metagenomics study of ticks from New South Wales in Australia (Gofton et al., 2022). The glycoprotein encoded by the largest contig of NTV shares 62% similarity to JMTV, ALSV and YGTV. Together, these examples represent only a small fraction of a diverse collection of viruses unearthed through next-generation sequencing (NGS).

NGS allows the detection of known and novel viruses from a wide range of sample types without requiring *a priori* knowledge derived from previous analyses, a feature that renders it suitable to study emerging and/or rare viruses (Roux et al., 2021). In this context, important reservoirs of viruses with high zoonotic potential, such as mosquitoes, ticks, rodents, and bats, are targeted for environmental surveillance. Notably, a study investigating the virome of 220 invertebrate species found 1,445 novel RNA viruses, highlighting the enormous variety of unknown and poorly characterised viruses in the environment (Shi et al., 2016a). Since most epidemics/pandemics caused by viruses have a zoonotic origin, one major goal of metagenomic surveillance is the timely identification of novel viruses, as well as their natural reservoirs, to enable an appropriate and expedient response from global health decision-makers during ongoing outbreaks.

6. Current state of arthropod-borne virus research in Portugal

Novel tick-borne viruses are expected to emerge and currently known agents may change their spatio-temporal distribution, enabled by anthropogenic and climatic factors acting on a global scale (Vayssier-Taussat et al., 2015). In Portugal, a diverse assemblage of RNA and DNA viruses circulates in arthropod vectors, including mosquitoes, ticks, and sandflies. A recent survey of mosquitoes collected in southern Portugal detected three lineages of insect-specific flaviviruses, a monophyletic cluster of viruses of the *Phenuiviridae* family (unassigned genera), and brevidensoviruses (*Parvoviridae*, *Densoviridae*), the latter two groups described for the first time in mosquitoes from Portugal (Silva et al., 2019). Sandfly fever Sicilian virus (SFSV), a sandfly-borne virus that causes febrile syndrome usually lasting two to

three days, is known to circulate in Portugal since its first serological detection in 1974 (Filipe, 1974), and was recently linked to the symptomatic infection of an eight-year-old boy in 2017 (Guerra et al., 2018). Human infections with the neurotropic sandfly-borne Toscana virus (TOSV) have also been reported, both in tourists visiting the country and in local residents (Ehrnst et al., 1985; Santos et al., 2007; Schwarz et al., 1995). Two other sandfly-borne phleboviruses, Massilia and Alcube viruses, were isolated in 2007 from specimens collected at the very same location (Arrábida, southern Portugal), but any seroprevalence studies carried out to assess the pathogenicity of both these species were either negative or inconclusive (Amaro et al., 2022; Bichaud et al., 2016). Nonetheless, the co-circulation of these viruses raises concerns due to the possibility of reassortment during arthropod co-infection, potentially originating new viruses of unknown pathogenicity (Amaro et al., 2022).

7. Aims

Regarding the current state of tick-borne virus circulation in Portugal, surveys carried out in our laboratory at the Institute of Hygiene and Tropical Medicine (IHMT) in recent years have revealed a surprising diversity of phlebovirus sequences in three genera of ticks collected across the whole extent of the country, including the Atlantic islands of São-Miguel (Azores) and Madeira (Pereira et al, 2017; Pimentel et al., 2019). These sequences clustered in multiple genetic lineages, namely AnLuc, KarMa, and RiPar virus 1, which, together with some sequences retrieved from Spain, share a most recent common ancestor originating in the Middle-East (Pimentel et al., 2019). Still, the number of studies investigating the diversity of tick-borne viruses in Portugal remains scarce. Given that jingmenviruses (1) are widespread across the globe, including nearby countries like France and Turkey, the latter characterised by a temperate Mediterranean climate; and (2) are able to infect a wide diversity of tick species, we hypothesised that known or unidentified members of this viral group may circulate in Portugal. Therefore, the aim of this research project consisted of screening ticks collected in Portugal for Jingmen group viruses using a dedicated nested PCR protocol and *in-house* designed primers. In parallel to these assays, the same tick pools were screened for phleboviruses, both as a means to control for cDNA quality but also to further assess the current diversity of phleboviruses circulating in Portugal. In addition, taking advantage of an institutional collaboration with the Faculty of Biology and Biotechnology (University of Warmia and Mazury in Olsztyn), total cDNA extracts of *Ixodes ricinus* ticks from Poland were surveyed for viruses of the genus *Flavivirus*, which includes the prominent disease agent tick-borne encephalitis virus (TBEV) known to be endemic to this region. Finally, phylogenetic analysis of the resulting sequences was carried out to characterise their genetic diversity.

MATERIALS AND METHODS

1. Collection, characterisation, and processing of tick samples

1.1. Collection, characterisation, and homogenisation of tick samples from Portugal

For logistic convenience, adult ticks were collected in July 2021 in two locations, Vila Franca de Xira (Estremadura) and Grândola (Alentejo), with the GPS coordinates 38°50'59.2"N 8°58'26.5"W and 38°06'26.3"N 8°34'11.7"W, respectively. Sampling was carried out by flagging vegetation in sites where contact with animals was frequently reported. Tick samples were stored in 50 mL conical tubes and preserved at -80°C to avoid nucleic acid degradation. Individuals were identified under a stereomicroscope with the aid of taxonomic keys (Estrada-Peña et al., 2004) and pooled into groups of 10 in 1.5 mL Eppendorf tubes according to their species and sex, as well as collection date and location. All ticks were washed to remove external contaminants by adding 100 mL 70% ethanol to each tube and mixing gently. Samples were blotted in paper towel, placed in sterile 1.5 mL Eppendorf tubes containing 250 µL Dulbecco's modified Eagle's medium (DMEM) supplemented with 4.5 g/L glucose without L-glutamine (BioWhittaker), and subsequently homogenised by direct crushing with a bent P1000 pipette tip. After adding 200 µL DMEM, the crushed tick mixtures were centrifuged at 13,000 × *g* for 10 min at 4°C, and 200 µL of the clarified supernatant were utilised in the RNA extraction procedure, whereas the remaining volume (~200 µL) was stored at -80°C for eventual viral isolation in cell cultures.

1.2. Total RNA extraction from tick homogenates

Total RNA was extracted from tick homogenates using ZR Viral RNA Kit (Zymo Research) according to the manufacturer's guidelines. The entire procedure was performed on ice in a RNase-free environment. In 1.5 mL microcentrifuge tubes, 350 µL of ZR Viral RNA Buffer was added to 150 µL of tick homogenate and mixed by pipetting. The mixture was transferred to a Zymo-Spin™ IC Column previously placed in a collection tube, centrifuged at 13,000 × *g* for 1 min, and the flow-through discarded from the collection tube. Following the addition of 200 µL of wash buffer to the column, the mixture was centrifuged at 13,000 × *g* for 30 sec, the flow-through was discarded and this washing step was repeated one more time. The column was then centrifuged at 13,000 × *g* for 2 min to ensure complete removal of the wash buffer and placed in DNase/RNase-free tubes. After pipetting 20 µL of DNase/RNase-free water directly onto the column filter and letting the column stand at room temperature for 1 min, the RNA was eluted by centrifugation at 13,000 × *g* for 1 min. If not used immediately for cDNA synthesis, total RNA extracts were stored at -80 °C.

1.3. cDNA synthesis from total RNA extracts

The commercial NZY First-Strand cDNA Synthesis Kit (NZYTech, Portugal) was used to synthesise cDNA from total RNA extracts according to the manufacturer's guidelines. On ice, 10 µL NZYRT 2× Master Mix, 2 µL NZYRT Enzyme Mix and 8 µL total RNA extract were added to nuclease-free microcentrifuge tubes and gently mixed by pipetting. The mixture was placed in a T-100 thermocycler (Bio-Rad, USA) for cDNA synthesis. Cycling conditions encompassed an initial incubation step at 25 °C for 10 min, during which random hexamers annealed to the RNA template and acted as primers for cDNA synthesis by the reverse transcriptase. This was followed by incubation at 50 °C for 45 min, which allowed for optimal enzyme activity during cDNA polymerisation and encouraged RNA denaturation. After a final inactivation step at 85 °C for 5 min, the tubes were chilled on ice. The RNA template was then removed by adding 1 µL RNase H (from *E. coli*) and incubating at 37 °C for 20 min. If not used immediately, final cDNA extracts were stored at -20 °C.

1.4. Collection and processing of tick samples from Poland (available cDNA)

The entire process leading to cDNA synthesis from *Ixodes ricinus* ticks from Poland was performed prior to this project, in the context of an institutional collaboration with the Faculty of Biology and Biotechnology (University of Warmia and Mazury in Olsztyn). Tick collection was carried out between May and September of 2021 in urban and suburban areas of Olsztyn, the capital of the Warmia and Mazury region in north-eastern Poland. Questing ticks were collected between 09:00 and 16:00, using the standard flagging method, and preserved in stayRNA™ buffer (A&A Biotechnology, Gdynia, Poland). Tick sample processing began with the extraction of total RNA from single individuals using NZYol (NZYTech, Lisbon, Portugal) according to the manufacturer instructions, and RNA quantification by Qubit Fluorometric Quantitation (Thermo Fisher Scientific, Waltham, MA, USA). cDNA was synthesized from 50 ng of total RNA using the iScript cDNA Synthesis Kit (Bio-Rad, Hercules, CA, United States), following the manufacturer's protocol.

2. Design of primers for detection of the Jingmen virus group and PCR set-ups

2.1. Preliminary phylogenetic analysis of Jingmen virus group sequences

Due to their highly conserved nature, two distinct regions coding the NS3-like protein and the NS5-like protein, respectively, were selected for analysis as potential targets for primer design. A dataset containing reference sequences downloaded from GenBank was created for each of these target regions,

including partial and complete coding sequences with a minimum length of 1414 nucleotides. Sequence retrieval was direct (via accession number) or based on similarity searches using BLASTn or NCBI-Virus to fully encompass all Jingmen virus group lineages known to date. Multiple sequence alignments were created for each dataset using the iterative G-INS-I method as implemented in MAFFT version 7 (Katoh et al., 2002; Katoh et al., 2013), followed by edition with GBlocks (Castresana, 2000) to eliminate any non-conserved or ambiguous regions that could compromise the reproducibility of the phylogenetic analysis. The phylogenetic content of each set of aligned sequences was assessed by likelihood mapping (Strimmer & Haeseler, 1997) in TREE-PUZZLE 5.3 (Schmidt et al., 2002). Both datasets were characterised by high phylogenetic signals (91.02% and 91.69% of random sequence quartets totally resolved in the NS3 and NS5 datasets, respectively) and thus considered reliable for phylogenetic inference. Primer-orienting phylogenetic trees were constructed based on the Maximum Likelihood (ML) optimisation criterion with TIM2 + F + G4 as the best-fitting evolutionary model, as suggested by IQ-TREE 1.6.12 (Trifinopoulos et al., 2016). Phylogenetic reconstructions were carried out in IQ-TREE running on an Ubuntu server. The robustness of the tree topologies was quantified by bootstrap analysis with 1000 replicates, in which bootstrap values > 70% were considered significant. Trees were visualised with FigTree 1.3.1 (Rambaut, 2010).

The observed distribution of sequences into groups A, B and C (see FIGURE 9 in section 2 of *Results and Discussion*) guided the design of amplification primers, using lineage-specific unedited multiple sequence alignments. For this purpose, sequence MN095533 was excluded from the NS3 alignments, as well as MT822179 and MN095531 from the NS5 alignments, due to inconsistent topology as evidenced by non-significant bootstrap values.

2.2. Requirements for primer design

Primers were designed using a combined approach that included visual inspection of multiple sequence alignments and the use of dedicated online tools Primer Design-M (Yoon & Leitner, 2015), Multiple Primer Analyzer (ThermoFisher) and Oligo Analysis Tool (Eurofins Genomics). Requirements for primer design included: (1) a primer length between 19 and 30 nucleotides; (2) non-dimerization; (3) minimal primer complexity (i.e., number of degenerate positions); (4) and the generation of final (post-second round) overlapping DNA fragments with similar sizes between the different viral lineages (885 to 911 nucleotides). The region coding the NS3-like protein was selected over the one coding the NS5-like protein as the final target for primer design for better fitting the above-mentioned criteria.

2.3. Nested PCR set-up and visualisation of amplification products

A total of six sets of primers was selected for a nested PCR protocol to detect jingmenviruses (**TABLE 3**). Of these six sets, two targeted a particular viral lineage (A, B or C), with the first set used in the first round of amplification and the second set of primers used in the second round of amplification. Considering the number of primers used in a single multiplex PCR reaction, and accounting for the complexity of the template cDNA samples, non-specific hybridisations could potentially limit target amplification. Therefore, a touch-down PCR protocol was selected to increase both the specificity and sensitivity of the anticipated amplification. PCR set-up was defined according to primer melting temperatures, with the annealing temperature decreasing 1 °C every cycle in the first 10 cycles (**TABLE 4**). The thermal profiles were identical in both amplification rounds except for the annealing temperature, which started at 61 °C in the first round and 62 °C in the second round. Based on the outcomes of PCR optimisation tests using an artificial positive control (further explained in sections 2.4 and 2.5), assays were conducted using two separate approaches: (1) a multiplex amplification assay, with primers targeting all three lineages included in a single reaction mixture; and (2) a singleplex assay using only primers for the largest viral lineage, A. Successful amplification was expected to produce an amplicon of approximately 1100 bp (first round) or 900 bp (second round).

TABLE 3. **Primers designed for the detection of the Jingmen virus group by touch-down nested-PCR.** Primer positions and number of mismatches are relative to the sequences of reference for each respective lineage. T_m denotes the mean melting temperature of each primer at 50 nM NaCl.

Target lineage	PCR round	Primer	Primer sequence (5'→3')	Binding region (reference sequence)	Primer complexity	T_m (°C)	Number of mismatches			Expected amplicon size (bp)
							A	B	C	
A	First	Fo_NS3_A	AGAACCTCWCCRGGRGTKAGYGG	847–869 (MK721575)	32	62.47	0	3	0	1141
	First	Ro_NS3_A	AGGCACATGTTRGCCTCSAR	1969–1988 (MK721575)	8	58.45	0	7	2	
	Second	Fi_NS3_A	CAGGRCCYTAYCAYCARTATGAGAT	953–977 (MK721575)	32	56.84	0	2	2	885
	Second	Ri_NS3_A	GGGGTTATCATCCCCTTDGTKCC	1816–1838 (MK721575)	6	59.24	0	5	3	
B	First	Fo_NS3_B	CGCCAGCGATAAAGACCCTCA	828–848 (MW556732)	1	59.43	4	0	11	1118
	First	Ro_NS3_B	TTATCACCCCTTTCGTGCCGGAC	1924–1946 (MW556732)	1	61.37	7	0	5	
	Second	Fi_NS3_B	GTCGGACAACTCCTGGCGTGAGCGG	957–981 (MW556732)	1	67.13	3	0	5	885
	Second	Ri_NS3_B	GTGGTGACAACGCAGAGCCCCTTC	1819–1842 (MW556732)	1	64.14	3	0	5	
C	First	Fo_NS3_C	AGCCTGGGGAAGACCACCAG	775–794 (MN107155)	1	61.80	3	4	0	1139
	First	Ro_NS3_C	GATGGGGTTATGACTCCTTTYGT	1892–1914 (MN107155)	2	55.72	7	0	0	
	Second	Fi_NS3_C	CCGGRGTAAGCGGATCACCCYTGTTCG	940–956 (MN107155)	4	65.98	8	13	0	911
	Second	Ri_NS3_C	TCGAACACMGCATCCAGGTCATA	1829–1851 (MN107155)	2	59.13	7	9	0	

For the detection of members of the *Phenuiviridae* family, primer sets ppL1 and ppL2 targeting a portion of the L segment were combined in a single multiplex reaction, as originally performed by Pereira et al. (2017), under similar cycling conditions to those described by Matsuno et al. (2015) (**TABLE 4**; **TABLE 5**). Amplification products corresponded to fragments of approximately 500 bp.

A nested PCR with primer sets 1NS5F/1NS5Re (first round) and 2NS5F/2NS5Re (second round) targeting the NS5 gene was employed in the detection of members of the *Flavivirus* genus, as described

by Vázquez et al. (2012) (**TABLE 4**; **TABLE 5**). Successful amplification was expected to yield a 1019 bp fragment.

TABLE 4. Cycling conditions used for the detection of Jingmen group viruses, phleboviruses and flaviviruses.

Target viral group	Round	Step	Number of cycles	Temperature (°C)	Duration (s or min)
Jingmen virus group	First	Initial denaturation	1	95	3 min
		Denaturation	10	95	30 s
		Annealing		61 to 52 (-1 °C each cycle)	45 s
		Extension		72	1 min 15 s
		Denaturation	30	95	30 s
		Annealing		52	45 s
		Extension		72	1 min 15 s
		Final extension	1	72	7 min
		Hold	1	4	∞
	Second	Initial denaturation	1	95	3 min
		Denaturation	10	95	30 s
		Annealing		62 to 53 (-1 °C each cycle)	45 s
		Extension		72	1 min 15 s
		Denaturation	30	95	30 s
		Annealing		53	45 s
		Extension		72	1 min 15 s
		Final extension	1	72	7 min
		Hold	1	4	∞
Phlebovirus		Initial denaturation	1	95	2 min
		Denaturation	50	95	30 s
		Annealing		55	90 s
		Extension		72	45 s
		Final extension	1	72	5 min
		Hold	1	4	∞
Flavivirus	First	Initial denaturation	1	95	3 min
		Denaturation	40	94	1 min
		Annealing		50	4 min
		Extension		72	1 min
		Final extension	1	72	10 min
		Hold	1	4	∞
	Second	Initial denaturation	1	95	3 min
		Denaturation	40	94	1 min
		Annealing		50	3 min
		Extension		72	1 min
		Final extension	1	72	10 min
		Hold	1	4	∞

TABLE 5. Primers used for the detection of phleboviruses and flaviviruses.

Target viral group	Primer set	Primer	Primer sequence (5'→3')*	Binding region**	Expected amplicon size (bp)	Reference
Phenuiviridae (*Bandavirus, Phlebovirus, Uukuvirus*)	ppL1	TBPVL2759F	CAGCATGGIGGICTIAGAGAGAT	2786–2803	500	Matsuno et al., 2015
		TBPVL3267R	TGIAGIATSCCYTGCATCAT	3281–3300		
	ppL2	HRT-GL2759F	CAGCATGGIGGIYTIAGRGAAATYTATGT	2786–2814		
		HRT-GL3276R	GAWGTRWARTGCAGGATICCYTGCATCAT	3281–3309		
Flavivirus	1NS5F/1NS5Re	1NS5F	GCATCTAYAWCAYNATGGG	9035–9053	1019	Vàzquez et al., 2012
		1NS5Re	CCANACNYNRTTCCANAC	10129–10146		
	2NS5F/2NS5Re	2NS5F	GCNATNTGGTWYATGTGG	9103–9120		
		2NS5Re	CATRTCTTCNGTNGTCATCC	10103–10122		

*Nonstandard nucleotides are as follows; I, inosine; R, adenine (A) and guanine (G); S, G and cytosine (C); W, A and thymine (T); Y, T and C.

**Reference sequences: *Phenuiviridae* – nucleotide positions in the L segment RNA (cRNA) of Uukuniemi virus strain S23 (GenBank accession number D10759); *Flavivirus* – indicated positions correspond to the sequence of WNV strain NY99-flamingo382–99 (accession number: AF196835).

Reaction mixtures for all assays were composed of NZYTaq 2× Green Master Mix (NZYTech, Portugal), primers and nuclease-free H_2O, and prepared on ice in a laminar flow cabinet, with 5 µL of the cDNA extracts added as the last component of the mix in a separate room (**TABLE 6**). All amplification steps were performed in a T-100 thermocycler (Bio-Rad, USA). Non-template negative controls were used in each run to rule out the possibility of false-positive amplifications due to cross-contamination. The presence or absence of an amplification product was confirmed by amplicon visualisation on 1% (w/v) agarose gels stained with ethidium bromide (0.5 µg/mL). The gels were loaded with 4 µL of the first or second round PCR products, as well as 2 µL of NZYDNA Ladder VI (NZYTech, Portugal) molecular weight marker, then ran at 90 V for 1h and visualised using a UV-light-based Gel Doc imaging system (Bio-Rad, USA).

TABLE 6. Composition of the reaction mixtures used in the PCR assays to detect Jingmen group viruses, phleboviruses and flaviviruses.

PCR round	Component	Target viral group			
		Jingmen virus group		Phlebovirus	Flavivirus
		Multiplex (primer sets A, B, and C)	Singleplex (primer set A)		
First	NZYTaq 2× Green Master Mix	12.5 µL	12.5 µL	10 µL	10 µL
	Primers (10 pmol/µL)*	6 µL**	2 µL**	4 µL	4 µL
	Nuclease-free H_2O	1.5 µL	5.5 µL	1 µL	1 µL
	cDNA	5 µL	5 µL	5 µL	5 µL
	Reaction mixture volume	25 µL	25 µL	20 µL	20 µL
Second	NZYTaq 2× Green Master Mix	10 µL	10 µL		10 µL
	Primers (10 pmol/µL)*	6 µL**	2 µL**		4 µL
	Nuclease-free H_2O	2 µL	6 µL		5 µL
	First round product	2 µL	2 µL		1 µL
	Reaction mixture volume	20 µL	20 µL		20 µL

*total volume of all primers used in reaction; **primers of jingmenvirus at 20 pmol/µL

2.4. Development of a positive control for Jingmen virus group amplification

Given that access to a jingmenvirus isolate for amplification control purposes was unviable in the context of this study, an artificial positive control was designed to test for amplification performance and subsequently adjust any parameters to maximise amplification yield. This positive control consisted of a DNA fragment flanked by the target sequences for the lineage A set of primers, "mimicking" a viral isolate of lineage A (**FIGURE 8A**). A central region of "stuffer DNA" consisting of a 987-nucleotide fragment of *Bacillus subtilis* bacteriophage SPP1 genome was included to obtain a total fragment size of 1084 nucleotides, which is equivalent to the expected size of the amplicon when using a viral extract. Positive control constructs were created by PCR amplification of bacteriophage SPP1 lysate at 10^9 pfu/mL (accession number X97918) as a template using hybrid primers in which the 3′-end hybridises with the SPP1 genome (**FIGURES 8B and 8C**). The 5'-end of these hybrid primers corresponded to the lineage A primer sequences with the degenerate positions replaced by nucleotides that are complementary to single-base polymorphisms found in a representative viral sequence of lineage A2 (accession number KJ001581). During amplification, the DNA polymerase added regions of this representative viral sequence to both ends of the "stuffer" DNA, creating an artificial fragment that could anneal to (and potentially be detected by) the primer sets Fo_NS3_A/Ro_NS3_A and Fi_NS3_A/Ri_NS3_A.

PCR assays to create the artificial control were carried out in a total volume of 25 µL, using 12.5 µL NZYTaq 2× Green Master Mix (NZYTech, Portugal), 2 µL each primer (FoFiSpp1F and RoRiSpp1R) at 10 pmol/µL, 2 µL SPP1 genome, and 6.5 µL nuclease-free H_2O. A gradient PCR assay was conducted at three different temperatures, which consisted of the predicted optimal primer annealing temperature of 58 °C according to T_m Calculator (Thermo Fisher) output, and 2 °C above (60 °C) or below (56 °C) the optimal T_m. This temperature gradient allowed for the empirical determination of optimal primer annealing temperature, accounting for any variability resulting from differences in reagent and cofactor concentrations (e.g., DNA template, dNTPs, Mg^{2+}, K^+). PCR parameters consisted of: (1) an initial denaturation step at 95 °C for 3 min; (2) 35 cycles of denaturation at 94 °C for 30 s, annealing at 56/58/60 °C for 30 s, and elongation at 72 ◦C for 30 s; (3) a final 10 min extension step at 72 °C. The PCR was performed in a T-100 thermocycler (Bio-Rad, USA) and included a non-template negative control. Amplification yield was assessed through amplicon visualisation on 1% (w/v) agarose gel, using the same conditions described in section 2.3. Successful amplification of the positive control occurred at 56 °C, 2 °C below the predicted optimal primer annealing temperature, as demonstrated by the presence of a ≈1100 bp band in the agarose gel.

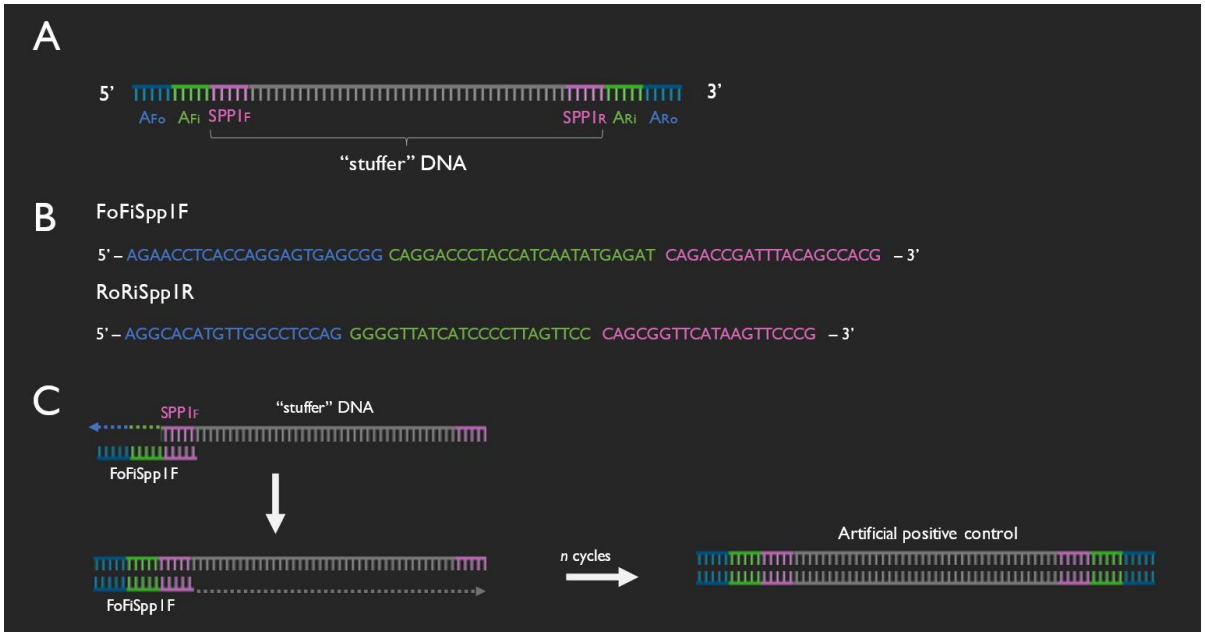

FIGURE 8. (A) Positive control, **(B)** hybrid primers and **(C)** mechanism of assembly of positive control. During the initial cycles of the PCR, the hybrid primers anneal their SPP1 portion (represented in purple in **B**) to the target regions in the SPP1 "stuffer" DNA ($SPP1_F$ and $SPP1_R$ in **A**, also in purple). As shown in **C**, the "stuffer" DNA fragment is gradually extended at the ends as the number of cycles increases and the DNA polymerase adds the target sequences of the lineage A primers (A_{Fi}/A_{Ri} in green and then A_{Fo}/A_{Ro} in blue, **A**) by complementarity to the corresponding regions in the hybrid primer.

2.5. Optimisation of the Jingmen virus group PCR protocol using in-house positive control

The PCR conditions defined for Jingmen virus group amplification in **TABLE 4** of section 2.3 were selected according to the outcome of preliminary assays using the artificial positive control designed in section 2.4, and in which three parameters were tested: (1) number of primer sets in a single reaction – multiplex (all three sets of primers) or singleplex (one set of primers); (2) starting annealing temperature – predicted optimal primer annealing temperature of 52 °C (first round)/ 53 °C (second round), or 2 °C above (54 °C / 55 °C) or below (50 °C / 51 °C) the optimal temperature; and (3) primer concentration – 10 pmol/µL or 20 pmol/µL. In all assays, reaction mix reagents were prepared as shown in **TABLE 6** of section 2.3, apart from the DNA template, which consisted of 2 µL of a 1:20 dilution of the positive control amplification product, and the volume of nuclease-free H_2O was also adjusted to obtain a final mixture volume of 25 µL (first round primers) or 20 µL (second round primers).

3. Fragment purification and molecular cloning

3.1. Fragment purification

The products of successful amplifications were purified using a commercial Zymoclean™ Gel DNA Recovery Kit (Zymo Research) according to the manufacturer's guidelines. DNA fragments were excised from the agarose gel using a microscope slide and transferred into previously weighed 1.5 mL microcentrifuge tubes (of weight M_{tube}). The agarose-filled tubes were weighed ($M_{tube+agarose}$) and the weight of the agarose slice calculated as $M_{agarose} = M_{tube+agarose} - M_{tube}$. Three volumes of Agarose Dissolving Buffer (ABD) were added per each volume of agarose (100 mg ≈ 100 µL) and the tubes were incubated at 55 °C until agarose was fully dissolved (approximately 15 min). Tube contents were pipetted into a Zymo-Spin™ Column previously placed in a collection tube, and centrifuged at 13,000 × *g* for 1 min. The flow-through was pipetted back into the column for a second passage in the same conditions. Flow-through was then discarded and columns washed twice with 200 µL DNA Wash Buffer by centrifugation at 13,000 × *g* for 30 s. After placing 6 µL of DNA Elution Buffer directly onto the column filter, the column was left to rest in a 1.5 mL microcentrifuge tube for 3 min to ensure complete hydration. Finally, the column was centrifuged at 13,000 × *g* for 2 min to elute the DNA. Purification yield was assessed by running 1 µL of the purification product in a 1% (w/v) agarose gel using the conditions described in section 2.3.

3.2. Molecular cloning of purified DNA fragments into plasmid vectors

The system used to clone amplification products was the commercial NZY-A PCR Cloning Kit (NZYTech, Portugal), based on the blue-white screening method for selection of bacterial colonies carrying recombinant plasmids. In summary, cells transformed with vectors containing the DNA fragment of interest produce white colonies due to the disruption of *lacZα*, a gene that codes for the *α*-peptide necessary for β-galactosidase function on *lacZΔM15* genetic backgrounds that only produce the β-galactosidase Ω fragment. When present in its functional form, as is the case when the cloning vector is not disrupted by the insert, the enzyme *β*-galactosidase cleaves the X-gal in the growth medium to produce a bright blue pigment that renders the bacterial colonies blue.

A mixture to ligate the PCR product into the plasmid vector was prepared according to kit instructions. After briefly vortexing each component, ligation mixtures were prepared on ice, in nuclease-free microcentrifuge tubes, using 5 µL NZY-A buffer, 1 µL NZY28-A vector, 3 µL PCR fragment, and 1 µL T4 DNA Ligase. Reactions were mixed thoroughly by pipetting, spun to collect the contents at the bottom of the tubes, and incubated overnight at 4 °C.

An adaptation of the protocol described by Chung et al. (1989) was used for bacterial cell transformation with recombinant plasmids, with all steps performed under sterile conditions. An isolated colony of competent *E. coli* NovaBlue (Novagen, USA) was inoculated in 3 mL liquid lysogeny broth (LB) supplemented with 12 µg/mL tetracycline and grown overnight at 37 °C, 220 rpm. Once saturated, 150 µL of the culture was pipetted into a Nephelo culture flask containing 15 mL of LB broth and grown at 37 °C, 220 rpm, until an OD_{600} of 0.4 was reached. The entire volume was then transferred into a 50 mL Falcon tube and centrifuged at 4 °C and 13,000 × *g* for 10 min. Flow-through was discarded and the pellet resuspended in 500 µL cold TSS (Transformation and Storage Solution). Half (i.e., 5 µL) of the ligation mixture prepared in the previous step was pipetted into 150 µL of the bacterial cell suspension, mixed gently, and incubated on ice for 30 min with occasional agitation. Transformation was attained by the heat shock method, in which samples were first placed in a water bath at 42 °C for 45 s, and then quickly back on ice for 5 min. To maximise competent cell recovery, 900 µL SOC (Super Optimal broth with Catabolite repression) medium was added before incubation at 37 °C for 1 h. Using sterile solid-glass beads, 200 µL of the bacterial suspension was plated on solid LB supplemented with ampicillin (100 µL/mL), X-gal (40 µg/mL), and IPTG (0.2 mM), followed by overnight incubation at 37 °C.

3.3. Plasmid DNA extraction by alkaline lysis

Alkaline lysis is routinely used to separate plasmid DNA from chromosomal DNA based on the former's smaller reduced size and supercoiled configuration (Birnboim & Doly, 1979). A minimum of 10 isolated white colonies were selected per sample/cloning experiment t, inoculated in 4 mL liquid LB supplemented with 4 µL ampicillin (100 mg/mL), and grown overnight at 37 °C and 220 rpm. Once saturated, 2 mL of the bacterial suspensions were centrifuged at 13,000 × *g* for 1 min. The pellets were resuspended in 250 µL TEG buffer (25 mM Tris-HCl pH 8, 1 mM EDTA, 1% glucose) and an equal volume of lysis buffer (0.2 M NaOH, 1.5% SDS) added to the mixture. The tubes were gently inverted to promote cell lysis and placed on ice until the mixtures turned translucid. With the addition of 250 µL potassium acetate 3M (pH 5.2), the chromosomal DNA (as well as other cell debris denatured by SDS) precipitated out of solution, whereas the plasmid DNA renatured in the supernatant. After centrifugation at 13,000 × *g* for 10 min, the supernatant was transferred to new 2 mL microcentrifuge tubes and 750 µL isopropanol added to precipitate the plasmid DNA, facilitated by gentle mixing and a centrifugation step at 13,000 × *g* for 30 min. The pellets were washed using 250 µL cold 70% ethanol, vortexed, and centrifuged at 13,000 × *g* for 5 min. Following blotting and drying in a vacuum desiccator (5 min, 45 °C), the pellets were resuspended in 40 µL TE buffer (10 mM Tris-HCl pH 8, 1 mM EDTA) supplemented with RNase A (50 µg/mL), and placed in a water bath at 37 °C for 30 min. Finally, 5 µL of the extraction products were subjected to electrophoresis on 0.8% agarose gel, where any clones

showing retarded migration in relation to the empty plasmid vector were expected to contain the DNA insert of interest, and thereby selected for sequencing.

3.4. Plasmid DNA purification

The selected recombinant plasmids were purified using chloroform ($CHCl_3$) to remove any traces of chromosomal DNA, cell debris and previously used reagents. Nuclease-free H_2O was added to the remaining extraction product to a total volume of 100 µL. Next, 100 µL $CHCl_3$ was emulsified into the mixture and centrifuged at 13,000 × *g* for 5 min, separating the mixture into an aqueous phase containing the DNA, and an organic phase containing the cell debris and proteins. The aqueous phase was then transferred to fresh tubes containing 10 µL NaOAc and an equal volume of isopropanol, with both reagents promoting the precipitation of the plasmid DNA after 5 min of incubation at room temperature and centrifugation at 13,000 × *g* for 30 min. The pellet was washed with 300 µL 70% ethanol, blotted, dried under vacuum and, lastly, resuspended in 20 µL nuclease-free H_2O. To assess the yield of the purification procedure, 1 µL of the extract was mixed with 2 µL of loading buffer, loaded into an 0.8% agarose gel and ran at 90V for about 20 min, which was enough time to allow the clear separation of any low-molecular weight contaminants like RNA, but not long enough that it would disappear completely from the gel.

4. Phylogenetic analysis of sequences

The purified recombinant plasmids were sent for Sanger sequencing at STABVIDA Lda. (Portugal), using primers that target the regions flanking the insert. The resulting sequences and corresponding chromatograms were processed and analysed on BioEdit Sequence Alignment Editor version 7.0.5.3 (Hall, 1999). Incomplete sequences, or those with an excess of ambiguous base calls and/or overlapping peaks in the chromatogram, were eliminated or, alternatively, re-sequenced for the purpose of building *contigs* from multiple nucleotide stretches with an overlapping region. Lastly, any regions corresponding to the vector or primer sequences were removed.

The processed sequence dataset was then merged with a dataset containing homologous sequences retrieved from NCBI, followed by a multiple sequence alignment, editing on GBLOCKS, and the construction of a phylogenetic tree based on the Maximum Likelihood (ML) method, as previously described in section 2.1.

Nucleotide identity and putative amino acid sequence analyses were conducted on MEGA 6 (Tamura et al., 2013) and BioEdit (Hall, 1999).

RESULTS AND DISCUSSION

1. Characterisation of tick samples collected in Portugal

A total of 715 ticks were collected in Vila Franca de Xira (EVOA) and Grândola (Herdade da Ribeira Abaixo), with a vast majority (98.6%) of the specimens identified as *Rhipicephalus bursa*, and only a small fraction as *Dermacentor marginatus* and *Hyalomma marginatum* (0.84% and 0.56%, respectively) (**TABLE 7**). Of these 705 *R. bursa* specimens, 350 (male and female) were further processed for RNA extraction and, together with 102 *Ixodes ricinus* and 15 *Dermacentor reticulatus* ticks from Poland, tested for the presence of jingmenviruses and phleboviruses (**TABLE 8**).

TABLE 7. Characterisation of tick samples collected in Portugal (EVOA and Grândola) during this study. In sex, "M" stands for male and "F" for female.

Collection date	Location	Species	Life stage	Sex	Counts
17/07/2021	EVOA	*Rhipicephalus bursa*	Adult	M	95
17/07/2021	EVOA	*Rhipicephalus bursa*	Adult	F	234
17/07/2021	EVOA	*Hyalomma marginatum*	Adult	M	2
17/07/2021	EVOA	*Hyalomma marginatum*	Adult	F	2
23/07/2021	EVOA	*Rhipicephalus bursa*	Adult	M	97
23/07/2021	EVOA	*Rhipicephalus bursa*	Adult	F	191
23/07/2021	EVOA	*Dermacentor marginatus*	Adult	M	0
23/07/2021	EVOA	*Dermacentor marginatus*	Adult	F	2
23/07/2021	Grandola*	*Rhipicephalus bursa*	Adult	M	34
23/07/2021	Grandola*	*Rhipicephalus bursa*	Adult	F	54
23/07/2021	Grandola*	*Dermacentor marginatus*	Adult	M	2
23/07/2021	Grandola*	*Dermacentor marginatus*	Adult	F	2
Total counts					715

* Precise location: Herdade da Ribeira Abaixo

TABLE 8. Number of individuals and respective pools for each tick species used in the PCR assays to detect Jingmen group viruses, phleboviruses and flaviviruses. NA (not applicable) indicates that survey was not carried out for that particular combination of virus group and tick species.

Tick species	Origin	Pool ID	Number of ticks per pool	Number of ticks (and pools) surveyed		
				Jingmen virus group	Phenuiviridae (*Bandavirus*, *Phlebovirus*, *Uukuvirus*)	*Flavivirus*
Ixodes ricinus	Poland	Ir1 - Ir40	3	87 (29)	102 (34)	33 (11)
Dermacentor reticulatus	Poland	Dr1 - Dr5	3	15 (5)	15 (5)	NA
Rhipicephalus bursa	Portugal	Rb1 - Rb35	10	350 (35)	350 (35)	NA

2. Preliminary phylogenetic analysis of Jingmen virus group sequences

In both phylogenetic trees based on the first and third segments (encoding proteins NSP1 and NSP2, respectively), viral sequences clustered into three major phylogenetic groups (**FIGURE 9**). The first group, referred to as group A in this study, represented most (> 80%) viral sequences known at the time of this experiment (late 2021) and was composed of JMTV strains. Group A was further sub-divided into two sub-groups, A1 and A2. Sub-group A1 included strains identified in China, Lao People's Democratic Republic, Uganda, and Brazil, while sub-group A2 consisted of strains from Trinidad and Tobago, French Antilles, Kosovo, Romania, and Turkey. The other two groups were composed mainly of JMTV-like viruses, with group B containing Yanggou tick virus (YGTV) sequences from China and Russia and group C including Alongshan virus (ALSV) sequences from China and Finland. Overall, sequences clustered into phylogenetic groups that matched those found in the literature, and where the clades designated A1, A2, and C in this analysis correspond to those named B, A, and C respectively, by Temmam et al. (2019) (see FIGURE 7 in section 4. of *Introduction*). Our clade C is also clustering as expected according to other analyses (see unnamed clade between clades B and C in FIGURE 7).

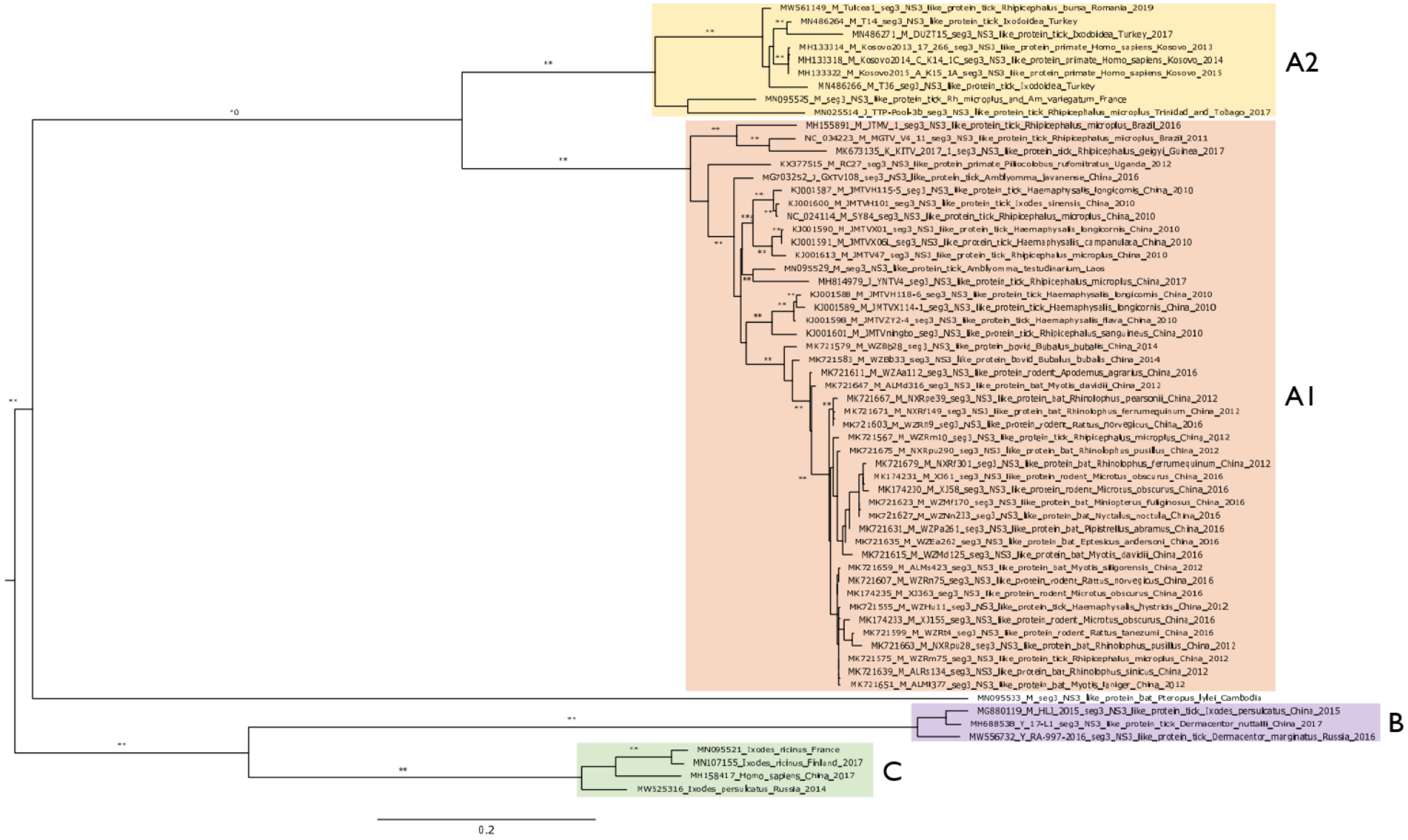

FIGURE 9. Primer-orienting phylogenetic analysis of jingmenviruses using RNA-dependent RNA polymerase (RdRp) complete coding sequences. Maximum likelihood (ML) rooted consensus tree based on 1,000 bootstrap replicates, with significant aLTR/bootstrap values represented as two asterisks (**) near the respective node (bootstrap ≥ 90% considered significant). Major clades A1, A2, B, and C colour-coded in red, yellow, purple and green, respectively.

3. Optimisation of the Jingmen virus group PCR protocol using *in-house* positive control

Three assays using the artificial positive control were performed to test for the influence of three parameters – multiplex/singleplex (assay 1), starting annealing temperature (assay 2), and primer concentration (assay 3) – in amplification performance. In assay 1, primer annealing temperatures were set to the predicted optimal values and the primer concentration used was 10 pmol/µL. The singleplex strategy clearly resulted in higher amplification efficiency, particularly when using the second-round primer set targeting lineage A (**FIGURE 10 – assay 1**), indicating a loss in detection sensitivity when combining multiple primers in a single amplification reaction due to competition or inhibition between primer sets. Assays 2 and 3 were performed under the same conditions as assay 1, except in assay 2 the starting primer annealing temperature was tested 2 °C above and below the predicted optimal temperature, whereas in assay 3 primer concentration was doubled to 20 pmol/µL. The 2 °C change in temperature appeared to slightly decrease amplification efficiency (**FIGURE 10 – assay 2**), however doubling primer concentration markedly increased amplification yield of the singleplex approach (**FIGURE 10 – assay 3**). All preliminary assays considered, it was decided to keep both multiplex and singleplex approaches for the experimental assays, as the former could potentially detect a greater variety of templates and the latter showed increased detection efficiency. The predicted optimal primer annealing temperatures remained unchanged, whereas primer concentration was doubled.

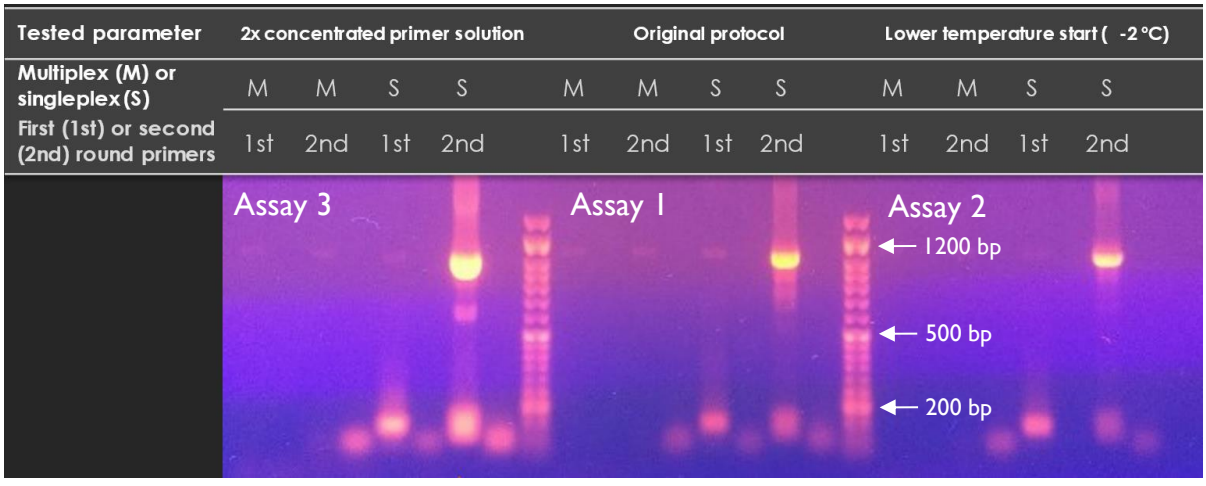

FIGURE 10. Optimisation of touch-down nested-PCR protocol for Jingmen tick virus detection using primers for three distinct clades (A, B, and C) and an artificial positive control. Higher temperature start (+ 2 °C) not shown in this figure but results were identical to those of assay 2. Note that 1100 bp and 900 bp (first and second round, respectively) amplicons were detected in all assays, with varying efficiency. NZYDNA Ladder VI (NZYTech, Portugal) used as molecular weight marker.

4. Jingmen group virus surveys in ticks from Portugal and Poland

No pools yielded an amplification product of 1100 bp (first round) or 900 bp (second round), as expected of a positive result for jingmenviruses (**TABLE 9**). These negative results could be related to several factors, such as low spatial and temporal coverage of the tick samples, as well as their taxonomic diversity. Due to constraints related to the current COVID-19 pandemic, tick collection in Portugal was limited to two locations and was carried out only during one week in July 2021. Jingmen virus group member prevalence in ticks is rather variable, with values as high as 11-55%, 75%, 75%, and 46% observed for different tick species across China, whereas in Russia prevalence was as low as 0.6%, 0.8%, 1.4% and 1.8% (Qin et al., 2014; Meng et al., 2019; Guo et al., 2020; Xu et al., 2021; Kholodilov et al., 2021). Two studies with a sample size of over 5,000 ticks belonging to more than 9 species, collected across multiple different sites and dates, only detected Jingmen tick virus in 3.1% and 3.9% of the tick pools (**TABLE 10**) (Kobayashi et al., 2021a; Dinçer et al., 2019). Interestingly, although JMTV-related sequences were detected in *I. ricinus* ticks from Alsace (France), no JMTV was identified in *I. ricinus* ticks from Ardennes, an area located only 200 km from the Alsace sampling area (Temmam et al., 2019). This study also reported the presence of JMTV in *Amblyomma* spp. ticks originating from Lao PDR, but not in *Haemaphysalis* spp. collected concomitantly in the very same location. The highly heterogeneous nature of jingmenvirus distribution across space, time, and tick species demonstrates the importance of rigorous, representative sampling.

TABLE 9. Number of tick pools that yielded amplification products in the PCR assays to detect Jingmen group viruses, phleboviruses and flaviviruses for three distinct tick species. NA (not applicable) indicates that survey was not carried out for the tick species in question.

Tick species	Origin	Pool ID	Number of ticks per pool	Number (and percentage) of positive pools		
				Jingmen virus group	Phenuiviridae (*Bandavirus*, *Phlebovirus*, *Uukuvirus*)	*Flavivirus*
Ixodes ricinus	Poland	Ir1 - Ir40	3	0/29 (0%)	4/34 (12%)	0/11 (0%)
Dermacentor reticulatus	Poland	Dr1 - Dr5	3	0/5 (0%)	0/5 (0%)	NA
Rhipicephalus bursa	Portugal	Rb1 - Rb35	10	0/35 (0%)	10/35 (29%)	NA

TABLE 10. Tick pools with detectable Jingmen virus sequences found in different studies.

Number of ticks	Number of tick species	Collection date	Number of collection sites	Number of positive individuals or pools	Prevalence	Reference
5008 (257 pools)	9	2018-2020	8 (Japan)	8 pools*	3.1%*	Kobayashi et al., 2021
7223 (630 pools)	>19	2013-2018	59 (Turkey)	25 pools	3.9%	Dinçer et al., 2019
360 (78 pools)	1	2014	2 (Russia)	10 pools*	13%*	Kholodilov et al., 2020
215	2	2012-2016	1 (China)	107 individuals	49.8%	Guo et al., 2020

*used high-throughput sequencing for detection

Another limitation to this study was the fact that the nested RT-PCR protocol for jingmenvirus detection was only optimised for an artificial positive control "mimicking" a viral isolate of lineage A (see FIGURE 8 in section 2.4. of *Materials and Methods*). Lineage A was selected over lineages B and C for encompassing the greatest number of viral sequences (see FIGURE 7 in section 1.4. of *Introduction*), but the possibility that any viral strains potentially circulating in Portugal cluster with other lineages cannot be ruled out. Ideally, viral isolates for all three lineages would have been used to optimise the nested RT-PCR protocol, but given the available capital and time frame to complete the study, only one artificial control was designed and tested for, with successful amplification observed nonetheless (see FIGURE 10 in section 3. of *Results and Discussion*). Indeed, to date, surveys for Jingmen-related viruses in ticks from Western European countries have only detected sequences belonging to lineage C (Colmant et al., 2022). In France, the closest neighbouring country for which Jingmen virus group detection studies in ticks have been carried out, the viral sequences described were grouped with Alongshan virus (ALSV) sequences of lineage C, two of which detected in Finland (see FIGURE 7 in section 1.4. of *Introduction*) (Kuivanen et al., 2019; Temmam et al., 2019). Similarly, ALSV was also detected in *Ixodes* spp. in Germany (Boelke et al., 2020; Colmant et al., 2022). Still, although not yet detected, it is feasible to hypothesise that JMTV circulates in Western European countries, even if in low prevalence, as its current distribution encompasses a wide range of host species and locations around the globe with varying climatic conditions. A JMTV sequence clustering with a Trinidad and Tobago strain of lineage B was discovered in *Aedes albopictus* mosquitoes from Italy (Parry et al., 2021), which raises concerns seen as this invasive mosquito is now fully established in Southern Portugal (Osório et al., 2020).

5. Phlebovirus surveys in ticks from Portugal and Poland

5.1. Detection of phlebovirus amplicons and molecular cloning

Despite the negative results for the detection of Jingmen and related viruses in ticks from Portugal and Poland, phleboviruses were detected in samples from both countries, as evidenced by the presence of a 500-bp band in the agarose gel containing the amplification products, as well as their clear association with other phlebovirus sequences in a phylogenetic tree (**TABLE 9; FIGURE 11; FIGURE 12**). This implies that the cDNA used in the concomitant Jingmen virus group surveys was present in sufficient quantity to exceed the minimum threshold for PCR detection, excluding poor cDNA quality as a possible cause for the negative results observed in this study.

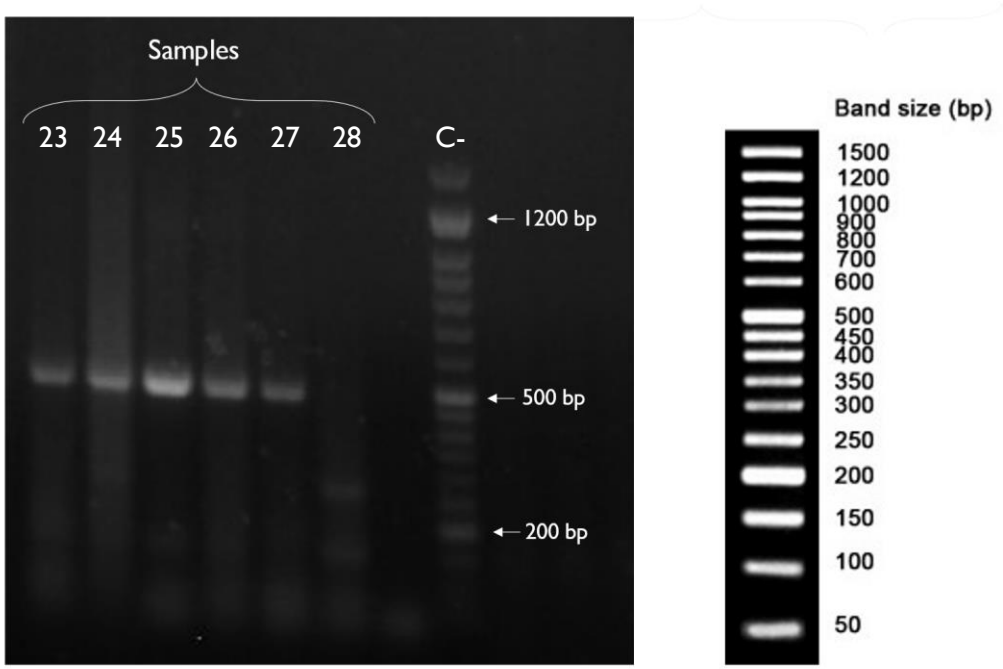

FIGURE 11. Example of electrophoretic analysis of the amplification products resulting from RT-PCR for phlebovirus in pooled samples 23-28 of *Rhipicephalus bursa* ticks collected in Portugal. NZYDNA Ladder VI (NZYTech, Portugal) used as molecular weight marker (shown on the right-hand side).

FIGURE 12A. Phylogenetic analysis of phlebovirus (*Bandavirus*, *Phlebovirus*, *Uukuvirus* and unassigned genera) L-segment 424-bp nucleotide sequences from *Rhipicephalus bursa* ticks collected in Portugal – collapsed format. Maximum likelihood (ML) rooted consensus tree based on 1,000 bootstrap replicates, with branch-specific aLTR/bootstrap values shown near the respective nodes (bootstrap ≥ 70% considered significant). Sequences obtained in this study presented in a collapsed format, marked with ◆, and supported by a bootstrap of 99%. Major phlebovirus phylogenetic groups highlighted in red (SFTS/Heartland group), green (Bhanja group), blue (Uukuniemi group), and yellow (Kaisodi group). Viral lineages identified by Pereira et al. (2017) and Pimentel et al. (2019) identified in purple.

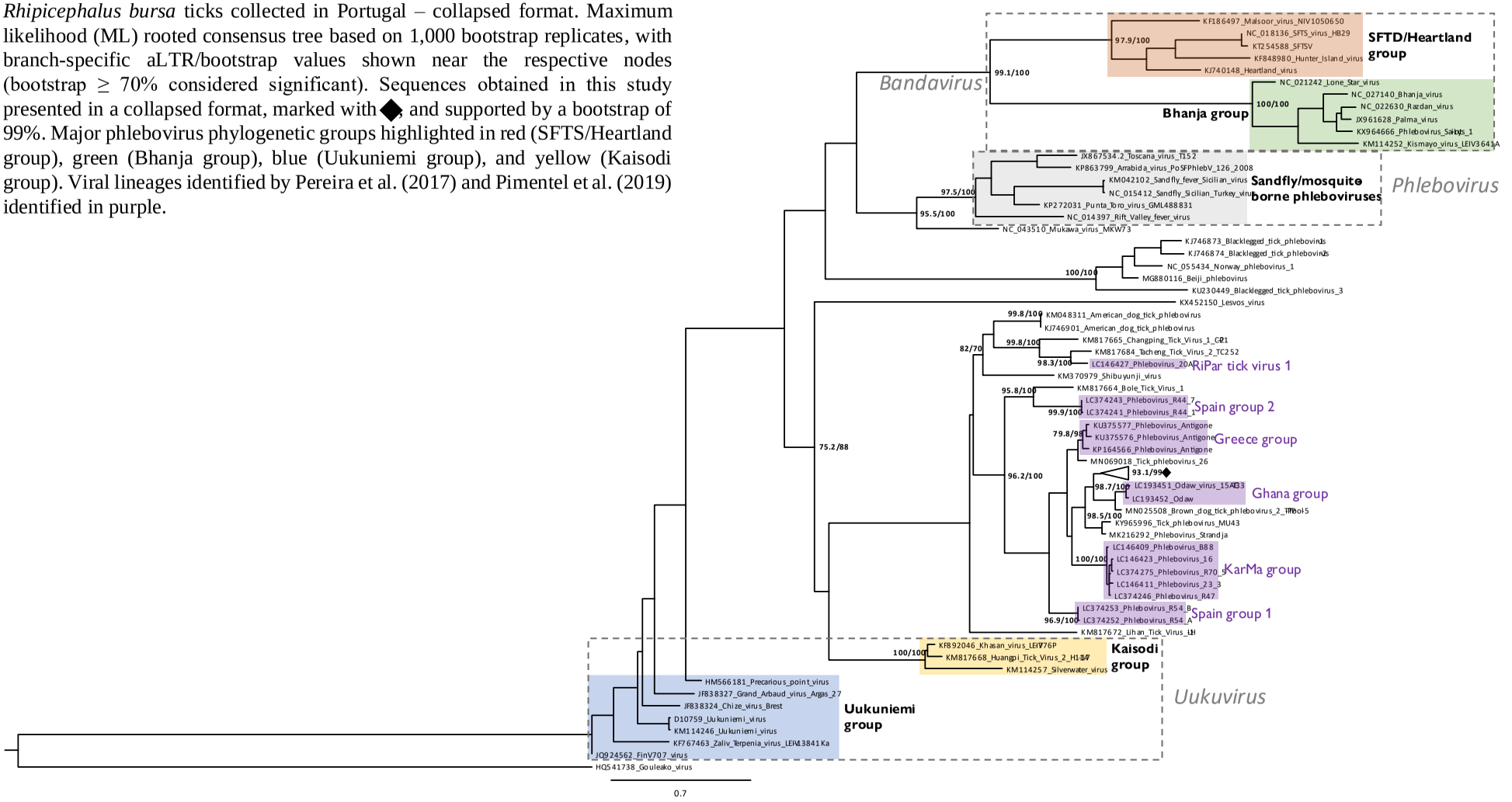

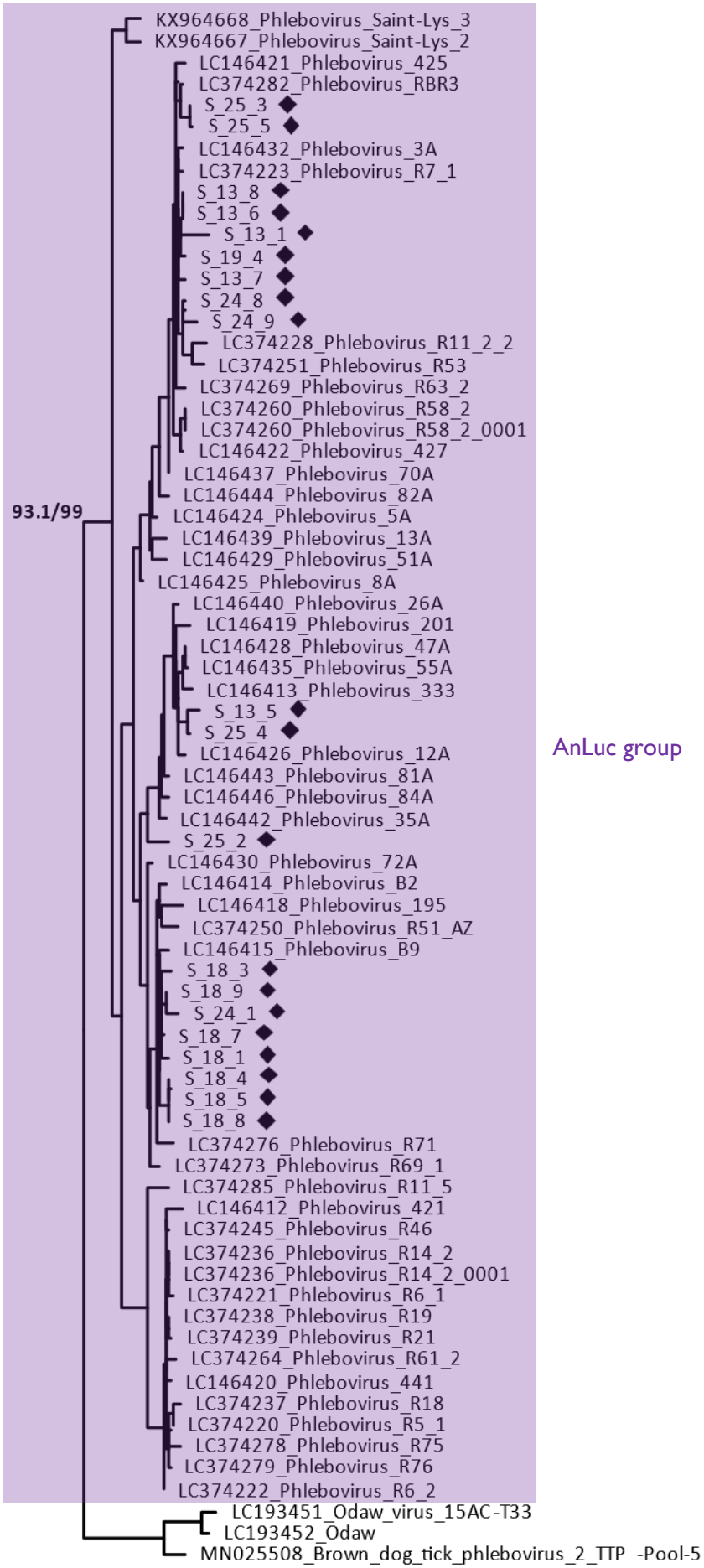

FIGURE 12B. Phylogenetic analysis of phlebovirus L-segment 424-bp nucleotide sequences from *Rhipicephalus bursa* ticks collected in Portugal, with a focus on the genetic group AnLuc. Maximum likelihood (ML) rooted consensus tree based on 1,000 bootstrap replicates, with the branch-specific aLTR/bootstrap value for the AnLuc group shown near the respective node (bootstrap ≥ 70% considered significant). Sequences obtained in this study, marked with ◆, belong to the AnLuc genetic group, supported by a bootstrap of 99%.

Following molecular cloning of the fragments into a plasmid vector (pNZY28-A), 2 to 8 clones per sample that displayed retarded migration in relation to the empty plasmid vector were selected for sequencing (**FIGURE 13**). Selected clones showed similar migration patterns across the agarose gel.

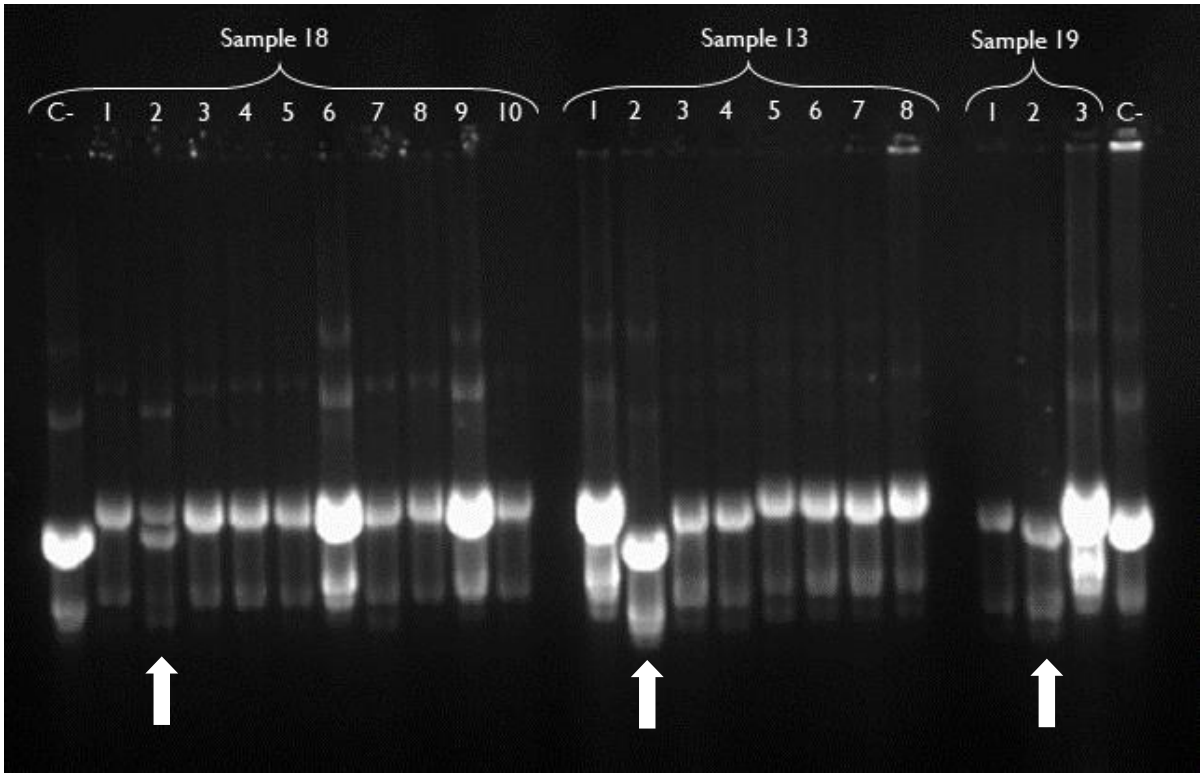

FIGURE 13. Electrophoretic analysis of the products that resulted from the molecular cloning of RT-PCR amplicons into plasmid vectors. "C-" represents lanes containing the empty plasmid, and lanes marked with an arrow represent plasmids that are unlikely to contain the insert.

5.2. Phylogenetic analysis of phleboviruses circulating in ticks from Portugal

Phlebovirus prevalence in pools of questing *R. bursa* ticks from Portugal was 29%, suggesting that their presence in these invertebrates is common, as observed in previous studies carried out in our laboratory (Pereira et al., 2017; Pimentel et al., 2019). The 20 sequences retrieved from five different tick pools (13, 18, 19, 24 and 25) all clustered with sequences from the AnLuc genetic lineage, supported by a significant bootstrap of 99% (**FIGURE 12**). These results were unsurprising, as the AnLuc group was originally comprised of sequences amplified from *R. sanguineus* s.l. and *R. bursa* specimens collected in Portugal (Pereira et al., 2017). All 20 sequences showed high intra-group similarity, with nucleotide sequence identities of at least 90%, and as high as 100% (**TABLE 11**). Similarity levels with previously discovered AnLuc sequences were also greater than 90% for most sequences, although no inferences regarding the genetic stability of the AnLuc group can be made due to the original studies being conducted 5 years apart from this one, which does not constitute a large enough temporal window to allow for an accurate assessment of genetic evolution across time and space.

TABLE 11. Nucleotide sequence identity values among phlebovirus sequences retrieved in *Rhipicephalus bursa* ticks collected in Portugal. Twenty different clones were sequenced from five different samples (13, 18, 19, 24 and 25).

	S_13_1	S_13_5	S_13_6	S_13_7	S_13_8	S_18_1	S_18_3	S_18_4	S_18_5	S_18_7	S_18_8	S_18_9	S_19_4	S_24_1	S_24_8	S_24_9	S_25_2	S_25_3	S_25_4	S_25_5
S_13_1	ID	90.0	96.6	95.9	96.6	94.1	93.6	93.8	93.8	94.5	94.1	95.2	95.7	94.5	95.2	94.1	90.5	93.8	88.9	93.3
S_13_5		ID	91.0	91.7	91.0	91.2	90.8	91.5	91.5	91.7	91.7	91.9	90.0	91.2	90.5	90.3	93.3	90.3	98.3	90.3
S_13_6			ID	98.8	100	91.7	91.2	91.5	91.5	92.2	91.7	92.9	99.0	91.9	98.5	97.4	93.8	97.1	90.3	96.6
S_13_7				ID	98.8	92.2	91.7	91.9	91.9	92.6	92.2	93.3	98.1	92.4	98.1	96.9	94.1	96.6	91.5	96.2
S_13_8					ID	91.7	91.2	91.5	91.5	92.2	91.7	92.9	99.0	91.9	98.5	97.4	93.8	97.1	90.3	96.6
S_18_1						ID	98.1	97.8	97.8	99.0	98.1	98.8	91.0	97.1	91.5	92.9	93.6	91.9	91.0	91.5
S_18_3							ID	97.4	97.4	98.5	97.6	98.3	90.5	96.6	91.0	92.4	93.1	91.5	90.5	91.0
S_18_4								ID	100	98.8	99.7	98.1	90.8	97.1	91.2	92.6	93.3	91.7	91.2	91.2
S_18_5									ID	98.8	99.7	98.1	90.8	97.1	91.2	92.6	93.3	91.7	91.2	91.2
S_18_7										ID	98.5	99.2	91.5	97.6	91.9	93.3	94.1	92.4	91.5	91.9
S_18_8											ID	98.3	91.0	97.4	91.5	92.9	93.6	91.9	91.5	91.5
S_18_9												ID	92.2	98.3	92.6	93.6	93.8	92.2	91.7	91.7
S_19_4													ID	91.2	98.1	96.6	93.1	96.6	89.6	96.2
S_24_1														ID	91.7	92.6	93.1	91.2	91.0	90.8
S_24_8															ID	98.1	93.6	98.1	90.0	97.6
S_24_9																ID	94.1	97.4	90.5	96.9
S_25_2																	ID	94.1	94.5	93.6
S_25_3																		ID	90.0	99.5
S_25_4																			ID	90.0
S_25_5																				ID

Clustering of both nucleotide and putative amino acid sequences occurred according to the major genetic groups defined by Matsuno et al. (2015) (Bhanja, Kaisodi, SFTS/Heartland, and Uukuniemi), and also followed the genetic lineage segregation patterns observed by Pereira et al. (2017) and Pimentel et al. (2019) (AnLuc, Greece, KarMa, Ripar tick virus 1, Spain group 1, and Spain group 2), which further supports the robustness of the phylogenetic analysis completed in this study (**FIGURE 12** and **FIGURE 14**). Likewise, high amino acid similarities of >95% were observed for the 20 sequences presently retrieved, as well as between these and the previously discovered AnLuc sequences.

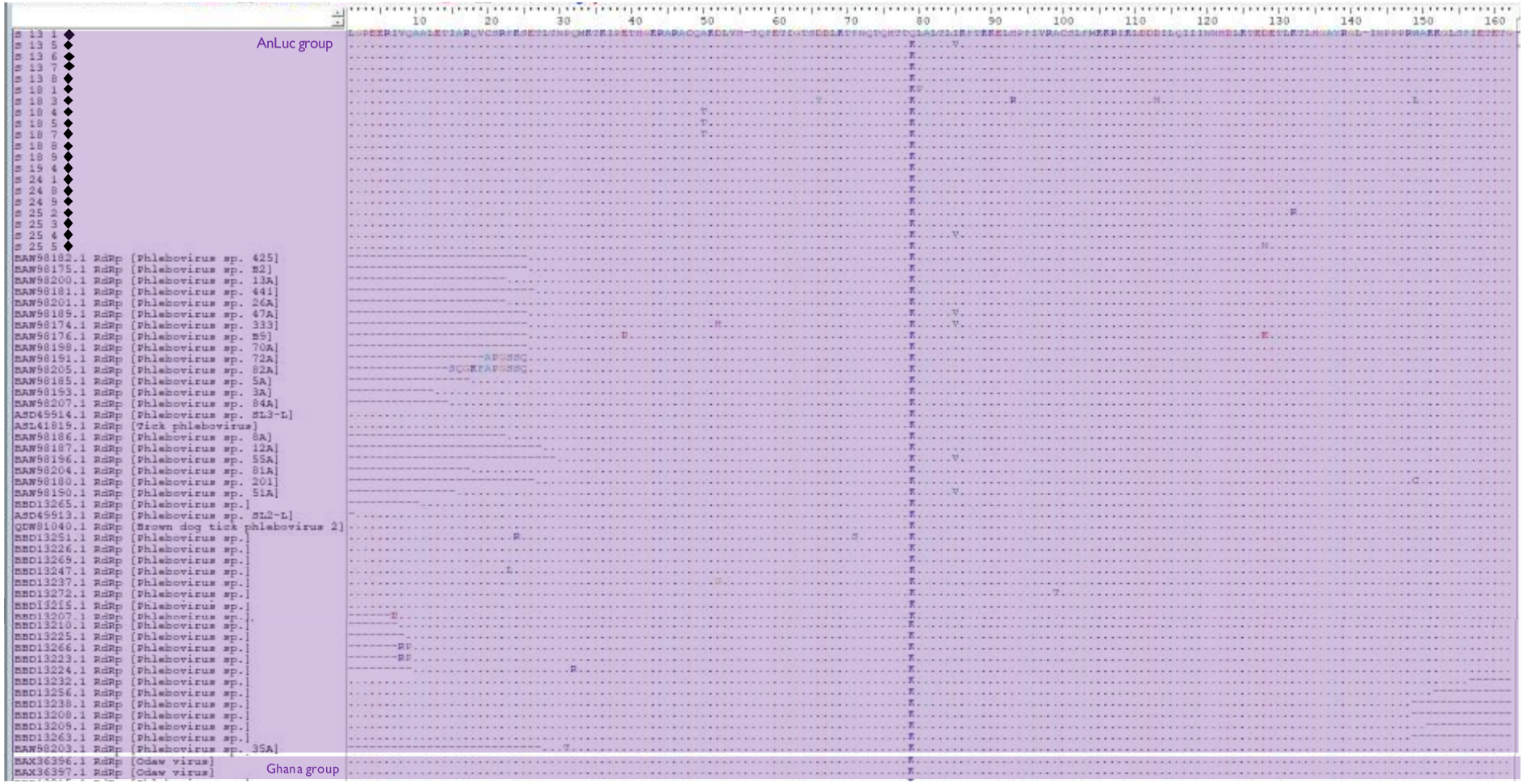

FIGURE 14. Characterisation of tick-borne phlebovirus sequences retrieved from *Rhipicephalus bursa* specimens collected in Portugal, based on the analysis of aligned putative amino acid sequences coded by 424-bp fragments of the L genomic segment. Sequences obtained in this study, marked with ◆, cluster with the AnLuc genetic group.

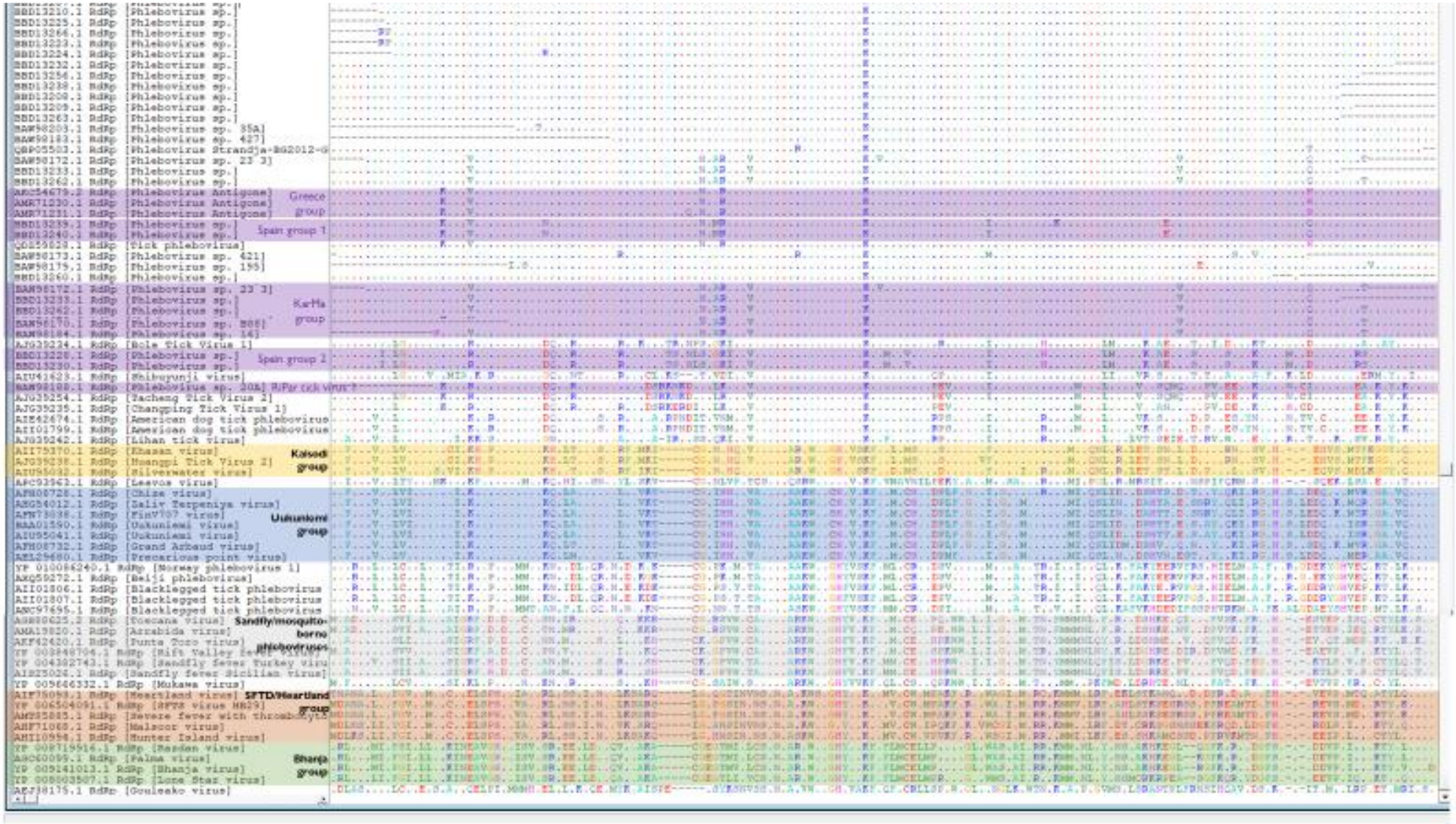
Greece group
Spain group 1
Karma group
Spain group 2
Kaisodi group
Uukuniemi group
Sandfly/mosquito-borne phlebovirus
SFTD/Heartland group
Bhanja group

5.3. Phylogenetic analysis of phleboviruses circulating in ticks from Poland

Phlebovirus prevalence in the analysed pools of questing *I. ricinus* ticks from Poland was 12%, lower than the prevalence of phleboviruses observed for the ticks from Portugal but still considered as a common occurrence. Previous analyses in Eastern Europe have shown that the minimum infection rate of Uukuniemi virus (UUKV) in *I. ricinus* from the Potepli region of Czech Republic is 3.95% (Kolman & Husova, 1971). Similarly, twelve strains of UUKV were isolated from the same tick species in Finland, with an infection rate of 0.5% (Lvov et al, 2015). Therefore, a prevalence of 12% is rather high relatively to other regions in Eastern Europe, and may reflect high endemicity of UUKV in *I. ricinus* in the Warmińsko-Mazurskie province. In any case, it is important to note that this could be an overestimation of the real prevalence, *since I. ricinus* pools were comprised of three individuals, and it is impossible to differentiate whether the positive result was derived from a single tick or multiple individuals within the same pool. Therefore, the actual prevalence of phlebovirus in *I. ricinus* from Poland may be slightly inferior to the values derived in this study.

Due to technical mishaps related to low efficiency of DNA recovery from agarose gels, only one sample out of 4 positive pools was successfully extracted and further sequenced for phylogenetic analysis. The sequence obtained in this study clustered with a UUKV Potepli63 strain from *I. ricinus* ticks collected in 1963 in Czech Republic, supported by a bootstrap of 99% (**FIGURE 15**). These results are consistent with the known distribution of UUKV in Central Europe, including Poland, where the same Potepli63 strain was isolated from *I. ricinus* ticks in 1970 (Wróblewska-Mularczykowa et al., 1970). Furthermore, the sequence isolated in this study shared 98.7% nucleotide identity with sequences KM114246 (Potepli63 strain, Czech Republic, 1963), MG969383 (Losov strain, Czech Republic, 2000), D10759 (S23 strain, Finland, 1973), and MG969386 (Lichnov strain, Czech Republic, 2004). Putative amino acid sequences derived from the nucleotide sequences obtained in this study also shared 100% identity with the amino acids derived from the same exact four UUKV strains (AIU95041, AWH61702, BAA01590, and AWH61706, respectively) (**FIGURE 16**). Considering that these four strains were isolated many years apart from each other, in different locations across Central/Northern Europe, such high values of sequence identity are not commonly observed for RNA viruses, which are characterised by fast rates of genetic evolution. However, UUKV appears to be one of those cases, with UUKV strains detected in Scandinavia almost 50 years apart showing >93% nucleotide identity across the entire M segment, and most mutations being silent, resulting in <2% amino acid difference (Mazelier et al., 2016). Other RNA viruses, like Tahyna orthobunyavirus (TAHV) and West Nile virus (WNV), have also been reported to have a relatively stable genome (Ergunay et al., 2015; Kilian et al., 2013).

FIGURE 15. Phylogenetic analysis of phlebovirus (*Bandavirus*, *Phlebovirus*, *Uukuvirus* and unassigned genera) L-segment 415-bp nucleotide sequences from *Ixodes ricinus* ticks collected in Poland. Maximum likelihood (ML) rooted consensus tree based on 1,000 bootstrap replicates, with branch-specific aLTR/bootstrap values shown near the respective nodes (bootstrap ≥ 70% considered significant). Sequence obtained in this study, marked with ◆, clusters together with a Uukuniemi virus (UUKV) of the Potepli63 strain, supported by a bootstrap of 99%. Major phlebovirus phylogenetic groups highlighted in red (SFTS/Heartland group), green (Bhanja group), blue (Uukuniemi group), and yellow (Kaisodi group).

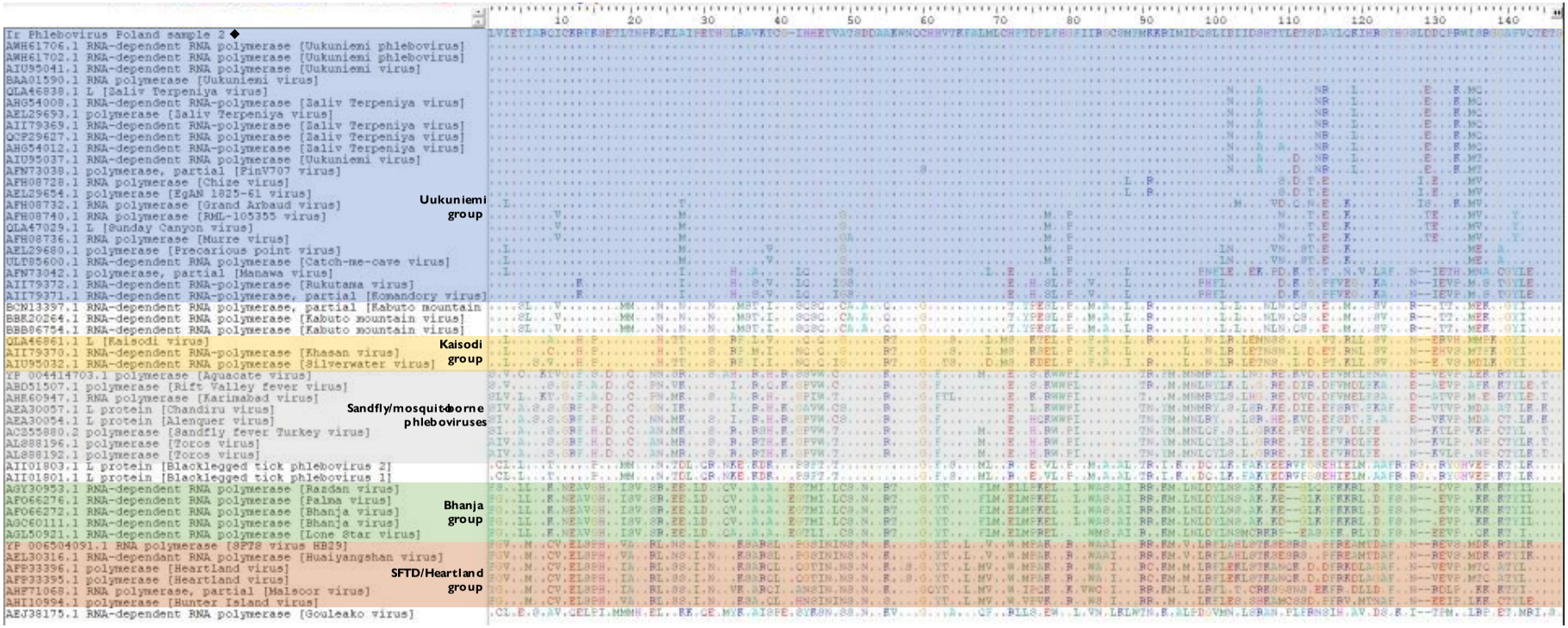

FIGURE 16. Characterisation of a tick-borne phlebovirus sequence retrieved from a *Ixodes ricinus* specimen collected in Poland, based on the analysis of aligned putative amino acid sequences coded by a 424-bp fragment of the L genomic segment. Sequence obtained in this study, marked with ◆, clusters with the Uukuniemi group.

6. Flavivirus surveys in ticks from Poland

No flavivirus were detected in 11 pools of 3 *Ixodes ricinus* individuals each (total of 33 ticks). Although tick-borne encephalitis is endemic in Central Europe, these results were not surprising, given that TBEV prevalence in questing ticks is known to be rather low across Europe (<1%) and geographically restricted to small foci (Rieille et al., 2017). In north-eastern Poland, the minimum infection rate of ticks with TBEV is 0.96% (Biernat et al., 2014; Brinkley et al., 2008; Rieille et al., 2017), and in the Warmińsko-Mazurskie province, which is considered highly endemic and where the tick samples for this study were collected, 1.55% (Biernat et al., 2014; Cisak et al., 2002; Kupča et al., 2010). Thus, a more thorough survey would have been preferable, including the processing of a higher number of ticks (at least 500), collected over a significantly wider geographical surface, and their distribution in pools of up to 10 individuals, allowing for enough genetic material from each individual. Nonetheless, given the medical importance of diseases transmitted by *I. ricinus*, such as tick-borne encephalitis and Lyme disease, surveys of this nature should be performed routinely, particularly in areas of risk for tick bites and high incidence of tick-borne diseases. Forest cover, for instance, is an important environmental determinant of the occurrence and activity of *I. ricinus*, as well as disease incidence, in eastern Poland (Zając et al., 2021), with correlations also reported from, Italy, and Switzerland (Perret et al., 2000; Tagliapetra et al., 2011). Surveillance data can be combined with habitat suitability modelling to assess current disease transmission risk, but also reveal possible future hotspot areas (Uusitalo et al., 2020).

FINAL CONSIDERATIONS

Given the current scenario of globalisation and climate change, the distribution of ticks, vertebrate hosts, and pathogens they carry is likely to shift in the upcoming decades. Epidemiological surveillance is therefore of the utmost importance to guide control measures and, with the aid of modelling-based predictive tools, map areas of high transmission risk. The most medically relevant tick-borne virus in central and eastern Europe is the tick-borne encephalitis virus (TBEV), with 10,000-12,000 human cases reported annually, and a case-fatality rate of up to 30% (ECDC, 2022b). In Poland, the province of Warmińsko-Mazurskie is recognised as highly endemic for TBEV (Biernat et al., 2014), although no pools of *Ixodes ricinus* yielded a positive detection for this virus, in a total of 660 individuals screened during the survey. These results could easily be attributed to the low prevalence (<1%) of TBEV in questing ticks (Rieille et al., 2017), but also reflect the geographic and/or seasonal heterogeneity that is characteristic of tick-borne virus distribution, even at the regional scale.

Besides notorious flaviviruses like TBEV, other neglected groups of tick-borne viruses, like those of the *Phenuiviridae* family, have attracted more attention in recent years with the discovery of two highly pathogenic species, thrombocytopenia syndrome virus (SFTSV) and Heartland virus (HRTV), in patients from China and the United States, respectively (Fang et al. 2015; Yu et al. 2011). SFTSV and HRTV cluster into the same phylogenetic group, but there are at least three other presently known groups of tick-borne phleboviruses. One of them is the non-pathogenic Uukuniemi group, named after its type species, the Uukuniemi virus (UUKV), which circulates in ticks from Scandinavia, Central and Eastern Europe, and Azerbaijan. In our study, the survey for phlebovirus in *I. ricinus* from Poland generated positive results in four of 34 tick pools, with sequences sharing 98.7% nucleotide identity with UUKV strains isolated between 1963 and 2004 in Czech Republic (Potepli63, Losov and Lichnov) and Finland (S23). The surprisingly high prevalence of 12%, when compared to previously reported values of 3.95% in Czech Republic (Kolman and Husova, 1971) and 0.5% in Finland (Lvov et al, 2015), may reflect a rather high endemicity in the Warmińsko-Mazurskie province. UUKV is known to circulate in Poland since at least 1970, the year it was first detected in this country (Wróblewska-Mularczykowa et al., 1970). Nonetheless, it is still interesting to observe that this virus has a remarkably stable RNA genome (at least for the RdRp coding region hereby analysed), as demonstrated by the high nucleotide identities between strains from 1963 and the sequences generated in the context of this study from specimens collected in 2021.

Tick-borne phleboviruses circulating in southern European countries do not fall into any of the four major phylogenetic groups (Bhanja, Kaisodi, SFTD/Heartland or Uukuniemi) described by Matsuno et al. (2015), but instead form multiple genetic lineages, namely AnLuc, KarMa, and RiPar virus 1, which, together with sequences retrieved from Spain, appeared to share a most recent common ancestor originating in the Middle-East (Pereira et al, 2017; Pimentel et al., 2019). The present survey for

phleboviruses in *Rhipicephalus bursa* ticks from the Vila Franca de Xira and Grândola regions of Portugal resulted in 10 positive pools in a total of 35 pools, with a high prevalence of 29%, in accordance with previous studies (Pereira et al, 2017; Pimentel et al., 2019). Likewise, all 20 nucleotide sequences shared 90-100% similarity with AnLuc sequences. To date, and to the best of our knowledge, only Pereira et al. (2017) have attempted to isolate and determine the pathogenicity of members of the AnLuc lineage, but these phleboviruses were unable to readily infect Vero (monkey kidney epithelial) or DH82 (canine macrophage) cells. Furthermore, the diverse nature of these genetic lineages, coupled with their co-circulation in some areas, raises the concern that re-assortment may occur during tick co-feeding, originating new viruses of unknown pathogenicity.

Although PCR-based approaches using targeted primers are routinely performed for their cost- and time-effectiveness, there is a general shift towards metagenomics-based screening, particularly when on the lookout for emerging and/or rare viruses for which there is little *a priori* information (Roux et al., 2021). Jingmen tick virus (JMTV), a novel virus genetically and functionally related to flavivirus, was first discovered in 2010 during a tick survey in China, has since been identified in all continents except Antarctica, and found to infect a broad range of tick species (at least 5 different genera), but also insects, scorpions, mammals, and even tortoises (Ogola et al., 2022; Paraskevopoulou et al., 2021). The closely related Alongshan virus (ALSV) was linked to cases of human febrile diseases in China and Kosovo (Li et al., 2015; Zhang et al, 2020), deeming this virus as a potential emerging threat to public health. In 2019, ALSV was identified together with TBEV in a metatranscriptomic survey of *I. ricinus* ticks collected in 2011 from south-eastern Finland (Kuivanen et al., 2019), highlighting the importance of molecular epidemiology surveys for tick-borne virus surveillance in Europe. In the context of the present study, no positive pools for jingmenviruses were detected in 29 pools of *I. ricinus* ticks from Poland and 35 pools of *R. bursa* ticks from Portugal. This could be related to the low spatial, temporal, and taxonomic diversity of the tick samples surveyed, limitations inherent to the targeted approach or, eventually, low prevalence or, simply, absence of this virus group in these regions. Other aspects to be elucidated in further studies regarding this unique flavi-like viral group include the role of migratory birds, bats, rodents, or domestic animals in the dissemination of jingmenviruses over continents (Temamm et al., 2019). Nevertheless, projects of exploratory nature such as this one, whether employing a targeted or NGS-based approach, have resulted in the discovery of a myriad of novel viruses in a surprising array of hosts. As the number of uncultivated viral genomes has surpassed that of isolated cultures, large virus sequencing surveys will accompany us in the future years.

REFERENCES

Adrion, E. R., Aucott, J., Lemke, K. W., & Weiner, J. P. (2015). Health care costs, utilization and patterns of care following Lyme disease. *PLoS ONE, 10*, e0116767.

Amaro, F., Zé-Zé, L., & Alves, M. J. (2022). Sandfly-borne phleboviruses in Portugal: four and still counting. *Viruses*, *14*, 1768.

Balducci, M., Verani, P., Lopes, M. C., & Nardi, F. (1970). Experimental pathogenicity of Bhanja virus for white mice and *Macaca mulatta* monkeys. *Acta Virologica*, *14*, 237–243.

Beauté, J., Spiteri, G., Warns-Petit, E., & Zeller, H. (2018). Tick-borne encephalitis in Europe, 2012 to 2016. *Eurosurveillance*, *23*, 1800201.

Beck, C., Jimenez-Clavero, M. A., Leblond, A., …, & Durand, B. (2013). Flaviviruses in Europe: complex circulation patterns and their consequences for the diagnosis and control of West Nile disease. *International Journal of Environmental Research and Public Health*, *10*, 6049–6083.

Bichaud, L., Dachraoui, K., Alwassouf, S., …, & Charrel, R. N. (2016). Isolation, full genomic characterization and neutralization-based human seroprevalence of Medjerda Valley virus, a novel sandfly-borne phlebovirus belonging to the Salehabad virus complex in northern Tunisia. *The Journal of General Virology*, *97*, 602–610.

Biernat, B., Cieniuch, S., & Stańczak. J. (2014). Detection of TBEV RNA in *Ixodes ricinus* ticks in north-eastern Poland. *Annals of Agricultural and Environmental Medicine, 21*, 689–692.

Birnboim, H. C. & Doly, J. (1979). A rapid alkaline extraction procedure for screening recombinant plasmid DNA. *Nucleic Acids Research*, *7*, 1513–1523.

Boelke, M, Kubinski, M., Dümmer, K., …, & Christine, S. (2020). Harz mountain virus, a new member of the zoonotic Alongshan virus group, is prevalent in ticks, tick saliva and game animals from Lower Saxony/Germany. In: 5. *Süddeutscher Zeckenkongress: Tagungsband*. Hohenheim: TiHo eLib. 46.

Brackney, D. E. & Armstrong, P. M. (2016). Transmission and evolution of tick-borne viruses. *Current Opinion in Virology, 21*, 67–74.

Brinkley, C., Nolskog, P., Golovljova, I., & Bergstro, T. (2008). Tick-borne encephalitis virus natural foci emerge in Western Sweden. *International Journal of Medical Microbiology*, *298*, 73–80.

Brinkmann, A., Dinçer, E., Polat C, …, & Ergünay, K. (2018). A metagenomic survey identifies Tamdy orthonairovirus as well as divergent phlebo-, rhabdo-, chu- and flavi-like viruses in Anatolia, Turkey. *Ticks and Tick-Borne Diseases*, *9*, 1173–1183.

Brites-Neto, J., Duarte, K. M. R., & Martins, T. F. (2015). Tick-borne infections in human and animal population worldwide. *Veterinary World*, *8*, 301–315.

Burger, T. D., Shao, R., Labruna, M. B., & Barker, S. C. (2014). Molecular phylogeny of soft ticks (Ixodida: Argasidae) inferred from mitochondrial genome and nuclear rRNA sequences. *Ticks and Tick-Borne Diseases*, *5*, 195–207.

Calisher, C. H. & Calzolari, M. (2021). Taxonomy of phleboviruses, emphasizing those that are sandfly-borne. *Viruses*, *13*, 918.

Castresana, J. (2000). Selection of conserved blocks from multiple alignments for their use in phylogenetic analysis. *Molecular Biology and Evolution*, *17*, 540–552.

CDC (2023). Uukuniemi. In: *Arbovirus Catalog*. http://wwwn.cdc.gov/arbocat/ [accessed on 30 March 2023].

CDC (2021). Babesiosis Graphs. Centers for Disease Control and Prevention. https://www.cdc.gov/parasites/babesiosis/data-statistics/graphs/graphs.html [accessed on 30 March 2023].

CDC (2022a). *Heartland virus disease*. Centers for Disease Control and Prevention. https://www.cdc.gov/heartland-virus/statistics/index.html [accessed on 30 March 2023].

CDC (2022b). Powassan Virus. Centers for Disease Control and Prevention. https://www.cdc.gov/powassan/index.html [accessed on 30 March 2023].

Chambers, T. J., Hahn, C. S., & Rice, C. M. (1990). Flavivirus genome organization, expression, and replication. *Annual Review of Microbiology*, *44*, 649–688.

Charrel, R. N., Fagbo, S., Moureau, G., … & Lamballerie, X. de. (2007). Alkhurma hemorrhagic fever virus in *Ornithodoros savignyi* ticks. *Emerging Infectious Diseases*, *13*, 153.

Chitimia-Dobler L, Mackenstedt U, & Petney TN. (2018). Transmission/Natural cycle. In: Dobler, G., Erber, W., Schimitt, H. J., editors. *Tick-borne Encephalitis (TBE)*. Singapore: Global Health Press Pte Ltd., 41–57.

Chitimia-Dobler, L., Mans, B. J., Handschuh, S., & Dunlop, J. A. (2022). A remarkable assemblage of ticks from mid-Cretaceous Burmese amber. *Parasitology*, *149*, 820–830.

Cisak, E., Chmielewska-Badora, J., Rajtar, B., Zwoliński, J., Jabłoński, L., & Dutkiewicz, J. (2002). Study on the occurrence of *Borrelia burgdorferi* sensu lato and tick-borne encephalitis virus (TBEV) in ticks collected in Lublin region (eastern Poland). *Annals of Agricultural and Environmental Medicine*, *9*, 105–110.

Colmant, A. M. G., Charrel, R. N., & Coutard, B. (2022). Jingmenviruses: ubiquitous, understudied, segmented flavi-like viruses. *Frontiers in Microbiology*, *13*, 997058.

Colwell, D.D., Dantas-Torres, F., & Otranto, D. (2011). Vector-borne parasitic zoonoses: emerging scenarios and new perspectives. *Veterinary Parasitology*, *182*, 14–21.

Dantas-Torres, F. (2018). Species concepts: what about ticks? *Trends in Parasitology*, 34, 1017–1026.

Dantas-Torres, F., Chomel, B. B., & Otranto, D. (2012). Ticks and tick-borne diseases: a One Health perspective. *Trends in Parasitology*, *28*, 437–446.

Dinçer, E., Hacıoğlu, S., Kar, S., …, & Ergünay, K. (2019). Survey and characterization of Jingmen tick virus variants. *Viruses*, *11*, 1071.

Dinçer, E., Timurkan, M. O., Oğuz, B., …, & Ergünay, K. (2022). Several tick-borne pathogenic viruses in circulation in Anatolia, Turkey. *Vector-Borne and Zoonotic Diseases*, *22*, 148–158.

Domínguez, M. C., Vergara, S., Gómez, M. C., & Roldán, M. E. (2020). Epidemiology of tick-borne relapsing fever in endemic area, Spain. *Emerging Infectious Diseases*, *26*: 849–856.

Duron, O., Sidi-Boumedine, K., Rousset, E., Moutailler, S., & Jourdain, E. (2015). The importance of ticks in Q fever transmission: what has (and has not) been demonstrated? *Trends in Parasitology*, *31*, 536–552.

ECDC (2022a). *Heartland virus disease*. Centers for Disease Control and Prevention. https://www.ecdc.europa.eu/en/crimean-congo-haemorrhagic-fever/facts/factsheet [accessed on 30 March 2023].

ECDC (2022b). *Tick-borne encephalitis*. In: Annual epidemiological report for 2020. Stockholm: European Centre for Disease Prevention and Control.

Ecker, M., Allison, S. L., Meixner, T., & Heinz, F. X. (1999). Sequence analysis and genetic classification of tick-borne encephalitis viruses from Europe and Asia. *Journal of General Virology*, *80*, 179–185.

Ejiri, H., Lim, C.K., Isawa, H., …, & Sawabe, K. (2017). Isolation and characterization of Kabuto Mountain virus: a new tick-borne phlebovirus from *Haemaphysalis flava* ticks in Japan. *Virus Research*, *244*, 252–261.

Ehrnst, A., Peters, C. J., Niklasson, B., Svedmyr, A., & Holmgren, B. (1985). Neurovirulent Toscana virus (a sandfly fever virus) in Swedish man after visit to Portugal. *Lancet*, *1*, 1212–1213.

Emmerich, P., Jakupi, X., von Possel, R., …, & Schmidt-Chanasit, J. (2018). Viral metagenomics, genetic and evolutionary characteristics of Crimean-Congo hemorrhagic fever orthonairovirus in humans, Kosovo. *Infection, Genetics and Evolution, 65*, 6 –11.

Ergunay, K., Bakonyi, T., Nowotny, N., & Ozkul, A. (2015). Close Relationship between West Nile Virus from Turkey and Lineage 1 Strain from Central African Republic. *Emerging Infectious Diseases*, 21, 352–355.

Estrada-Peña, A., Bouattour, A., Camicas, J., & Walker, A. (2004). *Ticks of domestic animals in the Mediterranean region: a guide to identification of species*. Zaragoza: University of Zaragoza Pres, 128.

Fang, L. Q., Liu, K., Li, X. L., … & Cao, W. C. (2015). Emerging tick-borne infections in mainland China: an increasing public health threat. *The Lancet Infectious Diseases*, *15*, 1467–1479.

Filipe, A. R. (1974). Serological survey for antibodies to arboviruses in the human population of Portugal. *Transactions of the Royal Society of Tropical Medicine and Hygiene*, *68*, 311–314.

Fujii, H., Tani, H., Egawa, K., …, & Saijo, M. (2022). Susceptibility of type I interferon receptor knock-out mice to Heartland bandavirus (HRTV) infection and efficacy of favipiravir and ribavirin in the treatment of the mice infected with HRTV. *Viruses*, *14*, 1668.

Gaudreault, N. N., Maddenm, D. W., Wilson, W. C., Trujillo, J. D., & Richt, J. A. (2020). African swine fever virus: an emerging DNA arbovirus. *Frontiers in Veterinary Science*, *7*, 215.

Gern, L., Estrada-Peña, A., Frandsen, F., …, & Nuttall, P. A. (1998). European reservoir hosts of *Borrelia burgdorferi* sensu lato. *Zentralblatt für Bakteriologie, 287*, 196–204.

Global Lyme Alliance (2023). *About Lyme Disease*. Global Lyme Alliance. https://www.globallymealliance.org/about-lyme/ [accessed on 30 March 2023].

Gofton, A. W., Blasdell, K. R., Taylor, C., ..., & Smith, I. (2022). Metatranscriptomic profiling reveals diverse tick-borne bacteria, protozoans and viruses in ticks and wildlife from Australia. *Transboundary and Emerging Diseases*, *69*, e2389-e2407.

Gondard, M., Temmam, S., Devillers, E., …, & Moutailler, S. (2020). RNA viruses of *Amblyomma variegatum* and *Rhipicephalus microplus* and cattle susceptibility in the French Antilles. *Viruses*, *12*, 144.

Guerra, A. B., Gouveia, C., Zé, L., Amaro, F., Ferreira, G. C., & Brito, M. J. (2018). Prolonged febrile illness caused by Sicilian virus infection in Portugal. In: *Proceedings of the 36th Annual Meeting of the European Society for Paediatric Infectious Diseases*. Malmo, Sweden, 28 May–2 June 2018.

Guo, J. J., Lin, X. D., Chen, Y. M., ..., & Zhang, Y. Z. (2020). Diversity and circulation of Jingmen tick virus in ticks and mammals. *Virus Evolution*, *6*, veaa051.

Hall, T. A. (1999). BioEdit: a user-friendly biological sequence alignment editor and analysis program for Windows 95/98/NT. *Nucleic Acids Symposium Series*, *41*, 95-98.

Heinz, F. X. & Holzmann, H. (2001). Tick-borne encephalitis. In: Service, M. W., editor. *The Encyclopedia of Arthropod-Transmitted Infections*. Wallingford, UK: CABI Publishing, 507–512.

Hermance, M. E. & Thangamani, S. (2017). Powassan virus: an emerging arbovirus of public health concern in North America. *Vector-Borne Zoonotic Diseases*, *17*, 453–462.

Hubalek, Z. (1987a). Geographic distribution of Bhanja virus. *Folia Parasitologica*, *34*, 77–86.

Hubalek, Z. (1987b). Experimental pathogenicity of Bhanja virus. *Zentralblatt für Bakteriologie, Mikrobiologie und Hygiene A*, 266, 284–291.

ICTV (2022). *Current ICTV Taxonomy Release*. https://ictv.global/taxonomy [accessed on 30 March 2023].

Jahfari, S. & Sprong, H. (2016). Emerging tick-borne pathogens: ticking on Pandora's box. In: Mah, B., Van Wieren, S. E., Takken, W., & Sprong, H., editors. *Ecology and prevention of Lyme borreliosis. Ecology and control of vector-borne diseases*, volume 4. Wageningen: Wageningen Academic Publishers, 127–147.

Jia, N., Liu, H. B., Ni, X. B., ..., & Cao, W. C. (2019). Emergence of human infection with Jingmen tick virus in China: a retrospective study. *EBioMedicine*, *43*, 317–324.

Katoh, K., Misawa, K., Kuma, K., & Miyata, T. (2002). MAFFT: a novel method for rapid multiple sequence alignment based on fast Fourier transform. *Nucleic Acids Research*, *30*, 3059–3066.

Katoh, K. & Standley, D. M. (2013). MAFFT multiple sequence alignment software version 7: improvements in performance and usability. Molecular Biology and Evolution, 30, 772–780.

Kazimírová, M., Thangamani, S., Bartíková, P., ... & Nuttall, P. A. (2017). Tick-borne viruses and biological processes at the tick-host-virus interface. *Frontiers in Cellular and Infection Microbiology*, *7*.

Keirans, J. E., Clifford, C. M., Hoogstraal, H., & Easton, E. R. (1976). Discovery of *Nuttalliella namaqua* Bedford (Acarina: Ixodoidea: Nuttalliellidae) in Tanzania and redescription of the female based on scanning electron microscopy. *Annals of the Entomological Society of America*, *69*, 926–932.

Kholodilov, I. S., Belova, O. A., Morozkin, E. S., Litov, A. G., Ivannikova, A. Y., Makenov, M. T., ..., & Karganova, G. G. (2021). Geographical and tick-dependent distribution of flavi-like Alongshan and Yanggou tick viruses in Russia. *Viruses*, *13*, 458.

Kilian, P., Valdes, J. J., Lecina-Casas, D., Chrudimský, T., & Růžek, D. (2013). The variability of the large genomic segment of Ťahyňa orthobunyavirus and an all-atom exploration of its anti-viral drug resistance. *Infection, Genetics and Evolution*, *20*, 304–311.

Kivaria, F. M. (2006). Estimated direct economic costs associated with tick-borne diseases on cattle in Tanzania. *Tropical Animal Health and Production*, *38*, 291–299.

Kobayashi, D., Kuwata, R., Kimura, T., …, & Isawa, H. (2021a). Detection of jingmenviruses in Japan with evidence of vertical transmission in ticks. *Viruses*, *13*, 2547.

Kobayashi, D., Kuwata, R., Kimura, T., …, & Isawa, H. (2021b). Toyo virus, a novel member of the Kaisodi group in the genus *Uukuvirus* (family *Phenuiviridae*) found in *Haemaphysalis formosensis* ticks in Japan. *Archives of Virology*, *166*, 2751–2762.

Kolman, J. M. & Husova, M. (1971). Virus-carrying ticks *Ixodes ricinus* in the mixed natural focus of the Central European tick-borne encephalitis virus (CETE) and Uukuniemi virus (UK). *Folia Parasitologica*, *18*, 329–335.

Kolman, J. M., Malkova, D., & Smetana, A. (1966). Isolation of a presumably new virus from unengorged *Ixodes ricinus* ticks. *Acta Virologica*, *10*, 171–172.

Kuivanen, S., Levanov, L., Kareinen, L., ..., & Vapalahti, O. (2019). Detection of novel tick-borne pathogen, Alongshan virus, in *Ixodes ricinus* ticks, south-eastern Finland. *Eurosurveillance*, *24*, 1900394.

Kupča, A. M., Essbauer, S., Zoeller, G., …, & Dobler, G. (2010). Isolation and molecular characterization of a tick-borne encephalitis virus strain from a new tick-borne encephalitis focus with severe cases in Bavaria, Germany. *Ticks and Tick-Borne Diseases*, *1*, 44–51.

Kwak, J. E., Kim, Y. I., Park, S. J., …, & Park, S. H. (2019). Development of a SFTSV DNA vaccine that confers complete protection against lethal infection in ferrets. *Nature Communications*, *10*, 3836.

Labuda, M. & Nuttall, P. A. (2004). Tick-borne viruses. *Parasitology*, *129*, S221–S245.

Ladner, J. T., Wiley, M. R., Beitzel, B., …, & Palacios, G. (2016). A multicomponent animal virus isolated from mosquitoes. *Cell Host Microbe*, *20*, 357–367.

Li, A., Dai, X., Chen, L., ..., & Li, D. (2022). Immunogenicity and protective efficacy of an inactivated SFTS vaccine candidate in mice. *Biosafety and Health*, *4*, 45–52.

Li, C. X., Shi, M., Tian, J. H., …, & Zhang, Y. Z. (2015a). Unprecedented genomic diversity of RNA viruses in arthropods reveals the ancestry of negative-sense RNA viruses. *eLife*, *4*, e05378.

Li, Y., Zhou, H., Mu, D., Yin, W., & Yu, H. (2015b). Epidemiological analysis on severe fever with thrombocytopenia syndrome under the national surveillance data from 2011 to 2014, China. *Zhonghua Liu Xing Bing Xue Za Zhi*, *36*, 598–602.

Ličková, M., Fumačová Havlíková, S., Sláviková, M., Slovák, M., Drexler, J. F., & Klempa, B. (2020). Dermacentor reticulatus is a vector of tick-borne encephalitis virus. *Ticks and Tick-Borne Diseases, 11*, 101414.

Liu, Q., He, B., Huang, S. Y., Wei, F., & Zhu, X. Q. (2014). Severe fever with thrombocytopenia syndrome, an emerging tick-borne zoonosis. *The Lancet Infectious Diseases*, *14*, 763–772.

Lvov, D. K., Shchelkanov, M. Y., Alkhovsky, S. V., & Deryabin, P. G. (2015). Chapter 8 – Single-Stranded RNA Viruses. In: Lvov, D. K., Shchelkanov, M. Y., Alkhovsky, S. V., & Deryabin, P. G., editors. *Zoonotic Viruses in Northern Eurasia*. Academic Press, 135–392.

Mans, B. J., de Klerk, D., Pienaar, R., & Latif, A. A. (2011). *Nuttalliella namaqua*: a living fossil and closest relative to the ancestral tick lineage: implications for the evolution of blood-feeding in ticks. *PLoS ONE, 6*, e23675.

Mans, B. J., de Klerk, D., Pienaar, R., Castro, M. H. De, & Latif, A. A. (2012). The mitochondrial genomes of *Nuttalliella namaqua* (Ixodoidea: Nuttalliellidae) and *Argas africolumbae* (Ixodoidae: Argasidae): estimation of divergence dates for the major tick lineages and reconstruction of ancestral blood-feeding characters. *PLoS ONE, 7*, e49461.

Mansfield, K. L., Jizhou, L., Phipps, L. P., & Johnson, N. (2017). Emerging tickborne viruses in the twenty-first century. *Frontiers in Cell and Infection Microbiology, 7*, 298.

Marjelund, S., Tikkakoski, T. F., Tuisku, S., Tuisku, S. F., Raisanen, S., & Raisanen, S. (2004). Magnetic resonance imaging findings and outcome in severe tick-borne encephalitis. Report of four cases and review of the literature. *Acta Radiologica, 45*, 88–94.

Maruyama, S. R., Castro-Jorge, L. A., Ribeiro, J. M., ... & Miranda-Santos, I. K. (2014). Characterisation of divergent flavivirus NS3 and NS5 protein sequences detected in *Rhipicephalus microplus* ticks from Brazil. *Memórias do Instituto Oswaldo Cruz, 109*, 38 –50.

Matsuno, K., Weisend, C., Kajihara, M., …, & Ebihara, H. (2015). Comprehensive molecular detection of tick-borne phleboviruses leads to the retrospective identification of taxonomically unassigned bunyaviruses and the discovery of a novel member of the genus phlebovirus. *Journal of Virology, 89*, 594–604.

Mazelier, M., Rouxel, R. N., Zumstein, M., Mancini, R., Bell-Sakyi, L., & Lozach, P. Y. (2016). Uukuniemi virus as a tick-borne virus model. *Journal of Virology, 90*, 6784–6798.

McMullan, L. K., Folk, S. M., Kelly, A. J., …, Nichol, S. T. (2012). A new phlebovirus associated with severe febrile illness in Missouri. The New England Journal of Medicine, 367, 834–841.

Meng, F., Ding, M., Tan, Z., …, & Tu, C. (2019). Virome analysis of tick-borne viruses in Heilongjiang Province, China. *Ticks and Tick-Borne Diseases*, *10*, 412–420.

NYC Government (2023). *Rocky Mountain spotted fever*. NYC Government. https://www.nyc.gov/site/doh/health/health-topics/rocky-mountain-spotted-fever.page [accessed on 30 March 2023].

Ogola, E. O., Kopp, A., Bastos, A. D. S, …, & Tchouassi, D. P. (2022). Jingmen tick virus in ticks from Kenya. *Viruses, 14*, 1041.

Osório, H. C., Rocha, J., Roquette, R., ..., & Alves, M. J. (2020). Seasonal dynamics and spatial distribution of *Aedes albopictus* (Diptera: Culicidae) in a temperate region in Europe, Southern Portugal. *International Journal of Environmental Research Public Health*, *17*, 7083.

Palacios, G., Savji, N., Travassos da Rosa, A., ..., & Tesh, R. (2013). Characterization of the Uukuniemi virus group (Phlebovirus: Bunyaviridae): evidence for seven distinct species. *Journal of Virology*, *87*, 3187–3195.

Pang, Z., Jin, Y., Pan, M., Zhang, Y., Wu, Z., Liu, L., & Niu, G. (2022). Geographical distribution and phylogenetic analysis of Jingmen tick virus in China. *iScience*, *25*, 105007.

Paraskevopoulou, S., Käfer, S., Zirkel, F., …, & Junglen, S. (2021). Viromics of extant insect orders unveil the evolution of the flavi-like superfamily. *Virus Evolution, 7*, veab030.

Parry, R., James, M. E., & Asgari, S. (2021). Uncovering the worldwide diversity and evolution of the virome of the mosquitoes *Aedes aegypti* and *Aedes albopictus*. *Microorganisms*, *9*, 1653.

Peñalver, E., Arillo, A., Delclòs, X., ... & Pérez-de la Fuente, R. (2017). Parasitised feathered dinosaurs as revealed by Cretaceous amber assemblages. *Nature Communications*, *8*, 1024.

Pereira, A., Figueira, L., Nunes, M., ..., & Parreira, R. (2017). Multiple *Phlebovirus* (*Bunyaviridae*) genetic groups detected in *Rhipicephalus*, *Hyalomma* and *Dermacentor* ticks from southern Portugal. *Ticks and Tick-Borne Diseases*, *8*, 45–52.

Perret, J. L., Guigoz, E., Rais, O., & Gern, L. (2000). Influence of saturation deficit and temperature on *Ixodes ricinus* tick questing activity in a Lyme borreliosis-endemic area (Switzerland). *Parasitology Research*, *86*, 554–557.

Pimentel, V., Afonso, R., Nunes, M., ..., & Parreira, R. (2019). Geographic dispersal and genetic diversity of tick-borne phleboviruses (*Phenuiviridae*, *Phlebovirus*) as revealed by the analysis of L segment sequences. *Ticks and Tick-Borne Diseases*, *10*, 942–948.

Poulos, C., Boeri, M., Coulter, J., Huang, L., Schley, K. & Pugh, S. J. (2022). Travelers' preferences for tick-borne encephalitis vaccination. *Expert Review of Vaccines*, *21*, 1495–1504.

Qin, X. C., Shi, M., Tian, J. H., …, & Zhang, Y. Z. (2014). A tick-borne segmented RNA virus contains genome segments derived from unsegmented viral ancestors. *Proceedings of the National Academy of Sciences of the United States of America*, *111*, 6744–6749.

Rambaut, A. (2010). *FigTree v1.3.1*. Institute of Evolutionary Biology, University of Edinburgh, Edinburgh. http://tree.bio.ed.ac.uk/software/figtree/ [accessed 30 March 2023].

Randolph, S. E. (2011). Transmission of tick-borne pathogens between co-feeding ticks: Milan Labuda's enduring paradigm. *Ticks and Tick-Borne Diseases*, *2*, 179–182.

Rieille, N., Klaus, C., Hoffmann, D., Péter, O., & Voordouw, M. J. (2017). Goats as sentinel hosts for the detection of tick-borne encephalitis risk areas in the Canton of Valais, Switzerland. *BMC Veterinary Research*, *13*, 217.

Rochlin, I. & Toledo, A. (2020). Emerging tick-borne pathogens of public health importance: a mini-review. *Journal of Medical Microbiology*, *69*, 781–791.

Roux, S., Matthijnssens, J., & Dutilh, B. E. (2021). Metagenomics in Virology. *Encyclopedia of Virology*, *2021*, 133–140.

Saikku, P. & Brummer-Korvenkontio, M. (1973). Arboviruses in Finland. II. Isolation and characterization of Uukuniemi virus, a virus associated with ticks and birds. *American Journal* of *Tropical Medicine* and *Hygiene*, *22*, 390–399.

Sameroff, S., Tokarz, R., Charles, R. A., … & Oura, C. (2019). Viral diversity of tick species parasitizing cattle and dogs in Trinidad and Tobago. *Scientific Reports*, *9*, 10421.

Santos, F. M. (2014). *PORDATA — Base de dados Portugal contemporâneo*. http://www.pordata.pt/Portugal/Doencas+de+declaracao+obrigatoria+casos+notificados-773 [accessed 30 March 2023].

Santos, L., Simões, J., Costa, R., Martins, S., & Lecour, H. (2007). Toscana virus meningitis in Portugal, 2002-2005. *Eurosurveillance*, *12*, E3–E4.

Schmidt, H. A., Strimmer, K., Vingron, M., & von Haeseler, A. (2002). TREE-PUZZLE: Maximum likelihood phylogenetic analysis using quartets and parallel computing. *Bioinformatics*, *18*, 502–504.

Schwarz, T. F., Jäger, G., Gilch, S., & Pauli, C. (1995). Serosurvey and laboratory diagnosis of imported sandfly fever virus, serotype Toscana, infection in Germany. *Epidemiology and Infection, 114*, 501–510.

Shah, K. V. & Work, T. H. (1969). Bhanja virus: a new arbovirus from ticks *Haemaphysalis intermedia* Warburton and Nuttall, 1909, in Orissa, India. The Indian Journal of Medical Research, 57, 793–798.

Sharma, D. & Kamthania, M. (2021). A new emerging pandemic of severe fever with thrombocytopenia syndrome (SFTS). *VirusDisease, 32*, 220–227.

Shi, M., Lin, X. D., Tian, J. H., …, & Zhang, Y. Z. (2016a). Redefining the invertebrate RNA virosphere. *Nature, 540*, 539–543.

Shi, M., Lin, X. D., Vasilakis, N., …, Zhang, Y. Z. (2016b). Divergent viruses discovered in arthropods and vertebrates revise the evolutionary history of the *Flaviviridae* and related viruses. *Journal of Virology, 90*, 659–669.

Shi, J., Hu, Z., Deng, F, & Shen, S. (2018). Tick-borne viruses. *Virologica Sinica*, *33*, 21–43.

Shi, J., Shen, S., Wu, H., Zhang, Y., & Deng, F. (2021). Metagenomic profiling of viruses associated with *Rhipicephalus microplus* ticks in Yunnan province, China. *Virologica Sinica*, *36*, 623–635.

Shi, J., Hu, S., Liu, X., …, Shen, S. (2017). Migration, recombination, and reassortment are involved in the evolution of severe fever with thrombocytopenia syndrome bunyavirus. *Infection, Genetics and Evolution, 47*, 109–117.

Silva, M., Morais, P., Maia, C., de Sousa, C. B., de Almeida, A. P. G., & Parreira, R. (2019). A diverse assemblage of RNA and DNA viruses found in mosquitoes collected in southern Portugal. *Virus Research, 274*, 197769.

Simmonds, P., Becher, P., Bukh, J., …, & Stapleton, J. (2017). ICTV Virus Taxonomy Profile: *Flaviviridae*. *Journal of General Virology*, *98*, 2–3.

Solomon, T., Hart, I. J., & Beeching, N. J. (2007). Viral encephalitis: a clinician's guide. *Practical Neurology*, *7*, 288.

Sood, S. K., O'Connell, S., & Weber, K. (2011). The emergence and epidemiology of Lyme borreliosis in Europe and North America. In: Sood, S.K., editor. *Lyme Borreliosis in Europe and North America: Epidemiology and Clinical Practice*. Hoboken, New Jersey: John Wiley & Sons, 1–35.

Spernovasilis, N., Markaki, I., Papadakis, M., Mazonakis, N., & Ierodiakonous, D. (2021). Mediterranean spotted fever: current knowledge and recent advances. *Tropical Medicine and Infectious Disease*, *6*, 172.

Stanojević, M., Li, K., Stamenković, G., …, & Zhang, Y. (2020). Depicting the RNA virome of hematophagous arthropods from Belgrade, Serbia. *Viruses*, *12*, 975.

Strimmer, K. & von Haeseler, A. (1997). Likelihood-mapping: A simple method to visualize phylogenetic content of a sequence alignment. *Proceedings of the National Academy of Sciences*, *94*, 6815–6819.

Sun, J., Min, Y. Q., Li, Y., …, & Ning, Y. J., (2021). Animal model of severe fever with thrombocytopenia syndrome virus infection. *Frontiers in Microbiology*, *12*, 797189.

Süss, J. (2003). Epidemiology and ecology of TBE relevant to the production of effective vaccines. *Vaccine*, *21*, S19–S35.

Tagliapietra, V., Rosà, R., Arnoldi, D., ..., & Rizzoli, A. (2011). Saturation deficit and deer density affect questing activity and local abundance of *Ixodes ricinus* (Acari, Ixodidae) in Italy. *Veterinary Parasitology*, *183*, 114–124.

Talagrand-Reboul, E., Boyer, P. H., Bergström, S., Vial, L., & Boulanger, N. (2018). Relapsing fevers: neglected tick-borne diseases. *Frontiers in Cell and Infection Microbiology*, *8*, 98.

Tamura, K., Stecher, G., Peterson, D., Filipski, A., & Kumar, S. (2013). MEGA6: Molecular Evolutionary Genetics Analysis version 6.0. *Molecular Biology and Evolution*, *30*, 2725–2729.

Temmam, S., Bigot, T., Chrétien, D., …, Eloit, M. (2019). Insights into the host range, genetic diversity, and geographical distribution of Jingmenviruses. *mSphere*, *4*, e00645-19.

Ternovoi, V. A., Gladysheva, A. V., Sementsova, A. O., …, & Loktev, V. B. (2020). Detection of the RNA for New Multicomponent Virus in Patients with Crimean-Congo Hemorrhagic Fever in Southern Russia. Vestnik Rossiiskoi Akademii Meditsinskikh Nauk, *75*, 129–134.

Trifinopoulos, J., Nguyen, L., Von Haeseler, A., & Minh, B. Q. (2016). W-IQ-TREE: A fast online phylogenetic tool for maximum likelihood analysis. *Nucleic Acids Research*, *44*, 232–235.

Tsergouli, K., Karampatakis, T., Haidich, A. B., Metallidis, S., & Papa, A. (2020). Nosocomial infections caused by Crimean-Congo haemorrhagic fever virus. *Journal of Hospital Infection*, *105*, 43–52.

Uusitalo, R., Siljander, M., Dub, T., ..., Vapalahti, O. (2020). Modelling habitat suitability for occurrence of human tick-borne encephalitis (TBE) cases in Finland. *Ticks and Tick-Borne Diseases*, *11*, 101457.

Vandegrift, K. J. & Kapoor, A. (2019). The ecology of new constituents of the tick virome and their relevance to public health. *Viruses*, *11*, 529.

Vayssier-Taussat, M., Cosson, J. F., Degeilh, ..., & Zylbermann, P. (2015). How a multidisciplinary 'One Health' approach can combat the tick-borne pathogen threat in Europe. *Future Microbiology*, *10*, 809–818.

Vázquez, A., Sánchez-Seco, M. P., Palacios, G., ..., & Tenorio, A. (2012). Novel flaviviruses detected in different species of mosquitoes in Spain. *Vector Borne Zoonotic Diseases*, *12*, 223–229.

Xu, X., Bei, J., Xuan, Y., … & Chen, Z. (2020). Full-length genome sequence of segmented RNA virus from ticks was obtained using small RNA sequencing data. *BMC Genomics*, *21*, 641.

Xu, B., Liu, L., Huang, X., & Chen, W. (2011). Metagenomic analysis of fever, thrombocytopenia and leukopenia syndrome (FTLS) in Henan Province, China: discovery of a new bunyavirus. *PLoS Pathogens*, *7*, e1002369.

Walter, C. T. & Barr, J. N. (2011). Recent advances in the molecular and cellular biology of bunyaviruses. *Journal of General Virology*, *92*, 2467–2484.

Wang, Z. D., Wang, B., Wie, F., …, & Liu, Q. (2019). A new segmented virus associated with human febrile illness in China. *The New England Journal of Medicine*, *380*, 2116 –2125.

WHO, 2023. *Tick-borne encephalitis*. World Health Organization. https://www.who.int/health-topics/tick-borne-encephalitis/#tab=tab_1 [accessed on 30 March 2023].

Wróblewska-Mularczykowa, Z., Sadowski, W., & Zukowski, K. (1970). *Folia Parasitologica*, *17*, 375.

Yoon, H. & Leitner, T. (2015). PrimerDesign-M: a multiple-alignment based multiple-primer design tool for walking across variable genomes. *Bioinformatics*, *31*, 1472–1474.

Yu, Z. M., Chen, J. T., Qin, J., …, & Zhang, Y.Z. (2020). Identification and characterization of Jingmen tick virus in rodents from Xinjiang, China. *Infection, Genetics and Evolution*, *84*, 104411.

Yu, X. J., Liang, M. F., Zhang, S. Y., …, & Li, D. X. (2011). Fever with thrombocytopenia associated with a novel bunyavirus in China. *The New England Journal of Medicine*, *364*, 1523–1532.

Zając, Z., Kulisz, J., Bartosik, K., Woźniak, A., Dzierżak, M., & Khan, A. (2021). Environmental determinants of the occurrence and activity of *Ixodes ricinus* ticks and the prevalence of tick-borne diseases in eastern Poland. *Scientific Reports*, *11*, 15472.

Zhang, X., Wang, N., Wang, Z., & Liu, Q. (2020). The discovery of segmented flaviviruses: implications for viral emergence. *Current Opinion in Virology*, *40*, 11–18.